

## Advances in high permeability polymeric membrane materials for CO<sub>2</sub> separations

Naiying Du,<sup>a</sup> Ho Bum Park,<sup>b</sup> Mauro M. Dal-Cin<sup>a</sup> and Michael D. Guiver<sup>\*ab</sup>

Received 14th September 2011, Accepted 31st October 2011

DOI: 10.1039/c1ee02668b

Global CO<sub>2</sub> emissions have increased steadily in tandem with the use of fossil fuels. A paradigm shift is needed in developing new ways by which energy is supplied and utilized, together with the mitigation of climate change through CO<sub>2</sub> reduction technologies. There is an almost universal acceptance of the link between rising anthropogenic CO<sub>2</sub> levels due to fossil fuel combustion and global warming accompanied by unpredictable climate change. Therefore, renewable energy, non-fossil fuels and CO<sub>2</sub> capture and storage (CCS) must be deployed on a massive scale. CCS technologies provide a means for reducing greenhouse gas emissions, in addition to the current strategies of improving energy efficiency. Coal-fired power plants are among the main large-scale CO<sub>2</sub> emitters, and capture of the CO<sub>2</sub> emissions can be achieved with conventional technologies such as amine absorption. However, this energy-consuming process, calculated at approximately 30% of the power plant capacity, would result in unacceptable increases in power generation costs. Membrane processes offer a potentially viable energy-saving alternative for CO<sub>2</sub> capture because they do not involve any phase transformation. However, typical gas separation membranes that are currently available have insufficiently high permeability to be able to process the massive volumes of flue gas, which would result in a high CO<sub>2</sub> capture. Polymer membranes highly permeable to CO<sub>2</sub> and having good selectivity should be developed for the membrane process to be viable. This perspective review summarizes recent noteworthy advances in polymeric materials having very high CO<sub>2</sub> permeability and good CO<sub>2</sub>/N<sub>2</sub> selectivity that largely surpass the separation performance of conventional polymer materials. Five important classes of polymer membrane materials are highlighted: polyimides, thermally rearranged polymers (TRs), substituted polyacetylenes, polymers with intrinsic microporosity (PIM) and polyethers, which provide insights into polymer designs suitable for CO<sub>2</sub> separation from, for example, the post-combustion flue gases in coal-fired power plants.

<sup>a</sup>Institute for Chemical Process and Environmental Technology, National Research Council Canada, Ottawa, Ontario, K1A 0R6, Canada. E-mail: michael.guiver@nrc-cnrc.gc.ca

<sup>b</sup>WCU Department of Energy Engineering, Hanyang University, Seoul, 133-791, Republic of Korea

### 1. Introduction

The emission of greenhouse gases (GHGs) mainly from fossil fuel combustion and other human economic and social activities has been escalating notably over the last century. The

#### Broader context

Global CO<sub>2</sub> emissions arising from escalating energy use, largely resulting from the combustion of fossil fuels, have increased steadily over the last century and have become one of the most challenging environmental issues. Technologies for CO<sub>2</sub> capture and storage (CCS) present some of the most promising and effective options for large-scale reductions in CO<sub>2</sub> emissions arising from global energy use. Among the CCS technologies being considered, polymeric membrane-based separation processes provide several advantages over other conventional separation techniques. However, the typical gas separation membranes currently available have insufficiently high permeability to be able to process the massive volumes of flue gas containing CO<sub>2</sub>. Polymeric membranes with very high permeability and good selectivity must be developed for the membrane process to be viable for CCS. This perspective review summarizes recent noteworthy advances in highly permeable and CO<sub>2</sub>-selective polymeric membrane materials that largely surpass the CO<sub>2</sub> separation performance of conventional polymer membranes, and provides an insight into polymer designs effective for CO<sub>2</sub> separation from large-volume gas streams.

atmospheric concentration of CO<sub>2</sub> has been increasing since the mid-19<sup>th</sup> century, and the annual rate is greater than ever, which is believed to be largely associated with current global warming.<sup>1</sup> To mitigate energy generation-related CO<sub>2</sub> emissions, the Intergovernmental Panel on Climate Change (IPCC) states in its third assessment report that the CO<sub>2</sub> emissions must be substantially reduced to achieve stabilization of the atmospheric CO<sub>2</sub> concentration during the 21<sup>st</sup> century.<sup>2</sup> Today, a large number of carbon sources such as fossil fuels, biomass energy facilities, chemical industries, natural gas processing, synthetic fuel plants, and fossil fuel-based hydrogen production plants result in the emission of megatons of CO<sub>2</sub> per day. Recent data show that fossil fuel-based power generation and industries, the main contributors to anthropogenic CO<sub>2</sub>, cumulatively released about 30.8 billion tons in 2009, which represents a reduction of only 1.3% compared with 2008, a record year. In addition, it is estimated that CO<sub>2</sub> emissions will increase by more than 3% in 2010.<sup>3</sup> This urgent situation is increasing the demand for more energy-efficient, cost-effective strategies for a massive reduction in CO<sub>2</sub> emissions. In a positive scenario, the use of carbon

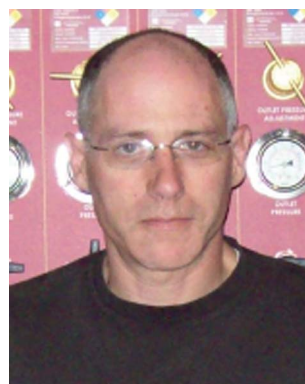
capture and storage (CCS) technologies in industry, fuel transformation and the power-generation sectors, which accounts for 14–19% of the emissions, would result in a total of 5.1 Gt to 10.4 Gt of CO<sub>2</sub> being captured.<sup>4</sup>

In the post-combustion carbon capture (PCCC) process, CO<sub>2</sub> can be captured from flue gases that contain 4% to 8% of CO<sub>2</sub> by volume for natural gas-fired power plants, and 12% to 15% by volume for coal-fired power plants.<sup>4</sup> Typically the CO<sub>2</sub> is captured through the use of solvents and subsequent solvent regeneration, sometimes in combination with membrane separation. Conventional absorption technology using amine-based solvents has been in use on an industrial scale for decades, but the challenge is to recover the CO<sub>2</sub> with a minimum energy penalty and at an acceptable cost (DOE target < \$20 per ton CO<sub>2</sub>).<sup>5</sup> Amine-based CO<sub>2</sub> capture has been estimated to consume approximately 30% of the power plant capacity, with corresponding power generation cost increases of 50–90%.<sup>6</sup> In a membrane-based separation process, there are challenges for treating the large volume of flue gases. The service conditions vary depending on the types of coal, steam cycles, and steam



**Naiying Du**

*Naiying Du is a Research Council Officer at the Institute for Chemical Process and Environmental Technology, National Research Council Canada (NRC). Her research focuses on the design of new polymeric materials with specific properties. She obtained her PhD at Graduate University of the Chinese Academy of Sciences, China. In 2005–2006, she worked as a postdoctoral fellow at McGill University and Case Western Reserve University.*



**Mauro M. Dal-Cin**

*Mauro Dal-Cin is a Research Officer at the National Research Council Canada (NRC) working on ultrafiltration and gas separations for industrial separations. He produces in-house membranes in flat sheet, hollow fibre and thin film composite formats. He obtained his BSc and MSc in Chemical Engineering at the University of Ottawa in 1985 and 1989 respectively.*



**Ho Bum Park**

*Ho Bum Park is an Associate Professor at the Department of Energy Engineering, Hanyang University, Seoul, Korea. He obtained his BSc, MSc and PhD from Hanyang University, Seoul, in 1996, 1998 and 2002 respectively. In 2005–2007, he worked as a postdoctoral fellow at the University of Texas at Austin. His membrane research, covering many years, is on the design and development of new advanced membrane materials for gas and liquid separation technologies and environmental green energy applications.*



**Michael D. Guiver**

*Michael D. Guiver is a Principal Research Officer at the National Research Council Canada (NRC), and a visiting professor at Hanyang University, Seoul, Korea. He obtained his BSc from London University in 1977, and his MSc and PhD from Carleton University, Ottawa, in 1980 and 1988 respectively. He is an Editor for the Journal of Membrane Science. He is known for his published work on polysulfone modification by lithiation, polymer electrolyte membranes for fuel cell application, and the development of high free-volume intrinsically microporous ladder polymers for membrane gas separation applications such as carbon dioxide capture.*

conditions in PCCC. A representative coal-fired flue gas composition is 12.5–12.8%, 6.2% H<sub>2</sub>O, 4.4% O<sub>2</sub>, 50 ppm CO, 420 ppm NO<sub>x</sub>, 420 ppm SO<sub>2</sub> and 76–77% N<sub>2</sub>. The pressure difference in the post-combustion is as low as 1.5 atm and the operating temperature is below 80 °C. Since the feed pressure is low and the gas volumes are very large, highly permeable membrane materials are preferred. The low CO<sub>2</sub> partial pressure gives rise to low driving forces for both permeation and separation. A combination of mild flue gas pressurization (<2 atm) and vacuum (0.2 atm) on the permeate side minimizes the energy requirements for flue gas pressurization and provides a feed/permeate pressure ratio sufficient for the desired separation. Energy savings are realized by using a slight vacuum on the permeate, because energy is expended on the CO<sub>2</sub>-rich permeate rather than on the feed composed primarily of N<sub>2</sub>.<sup>7</sup> In order to reduce the large membrane area required, membranes with very high CO<sub>2</sub> throughput (or flux) are necessary to compensate for the reduced driving force for permeation. Operation at low pressure also has the benefit of capital cost reductions for membrane housings.<sup>6</sup> An additional consideration is that polymer membranes should have tolerance to potentially harmful contaminants such as fly ash, SO<sub>2</sub>, NO<sub>x</sub>, water and trace metals that could reduce effectiveness and membrane lifetime.

In the past decades, membrane-based gas separations have been rapidly adopted industrially, because they offer advantages over conventional separation processes such as reduced environmental impact and lower capital and operating costs. The concept of membrane-based gas separation was originally proposed by Graham in 1866,<sup>8</sup> and was realized as a result of Loeb and Sourirajan's practical fabrication of asymmetric membranes in 1961.<sup>9,10</sup> The first membrane gas separation process was hydrogen recovery, commercialized in 1977.<sup>11</sup> The success inspired more awareness in this area, and led to different gas separation processes becoming commercially competitive with existing conventional technologies. Currently, membrane gas separation is utilized worldwide on an industrial scale for air separation (>99.5% nitrogen production and oxygen-enrichment), hydrogen recovery from ammonia purge stream, hydrocarbon/light gas separation, and CO<sub>2</sub> removal from natural gas.<sup>12,13</sup>

In the membrane separation process, a feed gas mixture is driven by a pressure difference across the membrane. A feed mixture is separated into one or more gases, thus generating a specific gas-enriched permeate or retentate. For gases, membranes are generally used in the form of thin-film composite flat sheet spiral wound modules or hollow fibre membranes. The latter are typically utilized for industrial applications because of their high surface area per unit volume.<sup>14</sup> To compete with well-established conventional separation processes and extend their applications further, however, polymer membranes with ultra-high permeance and good selectivity must be developed. This need has been reflected in recent research efforts to make high permeance membranes targeted for CO<sub>2</sub> capture from flue gases in coal-fired power plants.<sup>15</sup> The first CO<sub>2</sub> selective membranes, based on cellulose acetate and derivatives,<sup>16</sup> were demonstrated as early as the 1960s and the first industrial plants for CO<sub>2</sub> separation, using cellulose acetate membranes were installed in the 1980s. At the present time, there is much effort to develop CO<sub>2</sub> permeable, selective membrane materials and processes for

applications such as natural gas sweetening and biogas refinery (CO<sub>2</sub>/CH<sub>4</sub>), and CO<sub>2</sub> separation from post-combustion flue gases (CO<sub>2</sub>/N<sub>2</sub>) in coal-fired power plants.<sup>17</sup>

From a materials standpoint, polymers for gas separation membranes should meet the following requirements: good mechanical properties, thermal/chemical resistance, plasticization resistance and physical aging tolerance, which helps ensure adequate robustness and membrane lifetime under the challenging conditions encountered in practical usage.<sup>18,19</sup> A benefit of low pressure operation is that CO<sub>2</sub>-induced plasticization will not affect mixed gas selectivity. Other considerations for large scale industrial applications are important, such as cost-effectiveness and whether the membranes can be readily manufactured into membrane modules. For membrane gas separation in general, to achieve sufficient separation performance in a unit module, high permeability and high selectivity for a specific species in a mixture is required. However, in glassy or rubbery polymers, a well-known trade-off relationship is empirically observed between permeability ( $P$ ) and selectivity ( $\alpha$ ) for useful gas mixtures, *i.e.*, higher permeability is gained at the cost of lower selectivity and *vice versa*. This trade-off relationship can be represented by a double logarithmic plot of gas pair selectivity against the gas permeability of the faster species. Robeson demonstrated the empirical upper bounds in such plots in 1991<sup>20</sup> and revised the upper bounds in 2008 by incorporating new data.<sup>21</sup> Although many polymers have been investigated for gas separation membranes, few have been successfully commercialized, which can compete with existing separation technologies, partly due to this observed trade-off behavior. Therefore, it is highly desirable to expand the spectrum of high performance polymers having much higher gas permeability, while retaining adequate selectivity and fulfilling other requirements such as processability and long-term stability.

In this perspective review, some essential background knowledge on membrane gas separation and the importance of free volume in polymer design is first provided, and then recent advances in highly CO<sub>2</sub>-permeable polymers with good selectivity will be discussed.

## 2. General principles of membrane gas separation

In gas phase membrane applications, permeance and permeability are usually used as a measure of the gas transport rate. The permeance ( $Q$ ) is the pressure and area normalized parameter quantifying the productivity of an asymmetric membrane or thin film composite. The permeability ( $P$ ) is typically used with dense films where the thickness ( $\delta$ ) is well defined and is the permeance normalized by the thickness  $P = Q \times \delta$ . Units for the permeance are mol m<sup>-2</sup> s<sup>-1</sup> Pa<sup>-1</sup> or, more conveniently Gas Permeation Units (GPUs), where 1 GPU = 10<sup>-6</sup> cm<sup>3</sup> (STP) cm cm<sup>-2</sup> s<sup>-1</sup> cmHg<sup>-1</sup>. Units for permeability are mol m m<sup>-2</sup> s<sup>-1</sup> Pa<sup>-1</sup> or Barrer, where 1 Barrer = 10<sup>-10</sup> cm<sup>3</sup> (STP) cm cm<sup>-2</sup> s<sup>-1</sup> cmHg<sup>-1</sup>. Hence a polymer with a permeability of 1 Barrer will have a permeance of 1 GPU if the thickness is 1 micron. When mixed gases are used, the partial pressure difference of a gas is used.<sup>22</sup> The permeability of a polymer for gases is dependent on the membrane properties (*e.g.*, physical and chemical structures), the nature of the permeant species (*e.g.*, size, shape, and polarity), and the interaction between the membrane and

permeant species. Generally, the size and shape of a gas molecule determine its diffusional (kinetic) characteristics through a given polymer membrane, where the kinetic diameter, rather than the collision diameter, is the relevant property.<sup>23,24</sup> Recently, revised values for the kinetic diameters have been proposed.<sup>25,26</sup> The last factor is the interaction between the membrane and permeant, which is a thermodynamic characteristic related to the solubility of the gas in the polymeric membrane. As such, gas permeation behavior through polymer membranes is generally well-explained by the solution–diffusion mechanism.<sup>27,28</sup> That is, separation of gas pairs can be achieved not only by their diffusion through the dense polymeric matrix but also by the solubility of specific gases within the membrane, which relies on physiochemical interactions between the gas species and the polymers. The permeability coefficient (or permeability),  $P$ , of a penetrant is the product of the diffusion coefficient or diffusivity (kinetic parameter),  $D$ , and the solubility coefficient or solubility (thermodynamic parameter),  $S$ :

$$P = D \times S \quad (1)$$

In a membrane gas separation process, the permeant species are sorbed in the membrane at the higher pressure upstream side, diffuse through the membrane driven by the concentration gradient (measured by the partial pressure or fugacity difference), and then they desorb at the lower pressure downstream side. The solubility ( $\text{cm}^3(\text{STP}) \text{cm}^{-3} \text{cmHg}^{-1}$ ) is a measurement of the amount of gas sorbed by the membrane when equilibrated at a given gas pressure and temperature. Generally, penetrant solubility increases with increasing gas condensability (*i.e.*, higher critical temperature or high normal boiling point) and more favorable interactions with the polymer. The diffusivity ( $\text{cm}^2 \text{s}^{-1}$ ) is a concentration independent kinetic measure of penetrant transport rate through the membrane. Gas diffusivity can be enhanced by decreasing penetrant size, increasing polymer fractional free volume elements, and increasing polymer chain flexibility.<sup>17</sup> Membranes utilized in separations ideally need to possess both high selectivity and high permeability. The selectivity of the membrane to specific gas or liquid molecules is subject to the ability of the molecules to permeate through the membrane. The permselectivity (or ideal separation factor, determined from the permeation of individual pure gases),  $\alpha$ , is simply the ratio of two gases,  $A$  and  $B$ , being separated:

$$\alpha_{A/B} = \frac{P_A}{P_B} = \left[ \frac{D_A}{D_B} \right] \times \left[ \frac{S_A}{S_B} \right] \quad (2)$$

The permselectivity is also the product of the diffusivity selectivity and the solubility selectivity as shown in eqn (2). Robeson's empirically observed upper bounds were quantitatively predicted by Freeman<sup>29</sup> by using theoretical relationships for gas diffusivity and solubility based on the gas diameters, in eqn (1) and (2). The slope of the upper bounds was proven to be predicted by  $\lambda_{AB} = (d_A/d_B)^2 - 1$ , where  $d_A$  and  $d_B$  are the kinetic diameters,<sup>23,24</sup> or the revised diameters.<sup>25,26</sup>

Membranes are broadly classified as derived from rubbery or glassy polymers, depending on the polymer glass transition temperature.<sup>27</sup> For permanent gases (those having low gas-polymer interactions) in conventional glassy polymers, diffusivity selectivity dominates the permselectivity, with smaller gas

molecules diffusing faster than larger ones. Improvements in the gas separation performance of the polymeric membrane can be achieved by two different approaches;<sup>29,30</sup> by increasing the solubility of the faster gas in the membrane through changes in the polymer molecular structure or by increasing the diffusion of the faster gas. For condensable and hydrocarbon gases and organic vapors in rubbery polymers, solubility selectivity generally dominates and the gas solubility in the polymer matrix follows Henry's law and is linearly proportional to the partial pressure, or fugacity  $f$ .

$$C_D = K_D f \quad (3)$$

where  $C_D$  is the concentration of gas in the polymer matrix and is proportional through the Henry's constant ( $K_D$ ). On the other hand, glassy polymers generally exhibit more complex behavior. Below the glass transition temperature, glassy polymers do not reach thermodynamic equilibrium, which leads to inefficient chain packing and excess free volume in the polymeric matrix. In this case, Langmuir sorption also occurs, increasing the gas solubility. Therefore, the total concentration of sorbed gas  $C$  within glassy membranes in the dual-mode sorption model can be elucidated by a combination of Henry's law behavior,  $C_D$ , and Langmuir type behavior,  $C_H$ .

$$C = C_D + C_H = K_D f + C_H' \frac{bf}{1 + bf} \quad (4)$$

where  $C_H$  is the standard Langmuir relationship,  $C_H'$  is the maximum sorption capacity, and  $b$  is the ratio of rate coefficients of adsorption and desorption.

The maximum sorption capacity related to gas transport capacity in a glassy polymer can be also linked to the proportion and distribution of free volume elements. Free volume refers to the fraction of volume not occupied by the polymer molecular chain. When molecules are packed in a condensed phase, there is a limit to the packing density that can be achieved, so each molecule actually requires more space than its molecular volume. Typically the occupied volume is taken to include the van der Waals volume multiplied by a factor of 1.3, based on the packing density of a molecular crystal at 0 K. According to this concept, the disruption in chain packing is quantified by the fractional free volume (FFV) and is calculated using the following relationships:

$$V_f = (V_{sp} - 1.3V_w) \quad (5)$$

$$\text{FFV} = (V_f/V_{sp}) \quad (6)$$

where  $V_f$  is the free volume,  $V_{sp}$  is the specific volume, and  $V_w$  is the specific van der Waals volume calculated using the group contribution method of Bondi.<sup>31–33</sup> For a variety of glassy polymers, this approach gives values of  $V_f$  in the range of 0.11–0.23.<sup>34</sup> It indicates that glassy polymers contain a certain amount of FFV. If the proportion of free volume is increased to a large extent and it is effectively interconnected, the polymer is likely to exhibit high sorption capacity similar to that of microporous materials with high surface areas.<sup>35</sup> The free volume elements of glassy polymers may also be influenced by the solvent, casting and annealing conditions.



### 3. Recent advances in highly permeable polymers for CO<sub>2</sub> separation

Polymeric membrane-based separation processes provide several advantages over other conventional separation techniques. First, the membrane process is a viable energy-saving alternative for CO<sub>2</sub> separation, since it does not require a phase change of the gases. Second, the necessary process equipment is relatively simple with only a few moving parts such as compressors or vacuum pumps, compact, relatively easy to operate and control, and amenable to scale-up. It is envisioned that polymeric membranes can be effectively used to separate CO<sub>2</sub> from the gases of power generation point sources, if the polymeric membranes have high CO<sub>2</sub> permeance (>1000 GPU) and moderately good CO<sub>2</sub>/N<sub>2</sub> selectivity (>30). At CO<sub>2</sub>/N<sub>2</sub> selectivities above 30, increases in membrane CO<sub>2</sub> permeance are more important than further increases in selectivity.<sup>6</sup> Although many classes of polymers may be applied to membrane technology for CO<sub>2</sub> separation applications, such as polyamides,<sup>36</sup> polyimides,<sup>37</sup> polyacetylenes,<sup>38</sup> polycarbonates,<sup>39</sup> polyarylates,<sup>40</sup> poly(phenylene oxide)s,<sup>41</sup> poly(ethylene oxide)s,<sup>42</sup> polyanilines,<sup>43</sup> polysulfones<sup>44</sup> and polypyrrolones,<sup>45</sup> only a few have high CO<sub>2</sub> permeability (>100 Barrer).

Consideration must also be given to the ability to fabricate membranes with a thin gas separating layer: either the skin layer of an asymmetric membrane or the coating of a thin-film composite (TFC). A polymer separating layer with a 100 nm effective thickness and a permeability coefficient of 100 Barrer will have a permeance of 1000 GPU, while a 1000 Barrer polymer with a layer thickness of 4 microns will have a permeance of only 250 GPU. Commercial membranes with the highest CO<sub>2</sub> permeances reported to date have used both fabrication approaches.

Asymmetric hollow fibre membranes derived from cardo-polyimide PMBP64(4Me)-Br were reported by Kazama *et al.*<sup>46</sup> to have a CO<sub>2</sub> permeance of 1000–1300 GPU and a CO<sub>2</sub>/N<sub>2</sub> selectivity of 41. The dense film CO<sub>2</sub> permeability measured was 130 Barrer, with the same CO<sub>2</sub>/N<sub>2</sub> selectivity; hence the skin layer thickness of the fibre surface was reported by Kazama *et al.* to be about 100 nm. Membrane Technology Research Inc. (MTR Inc., Menlo Park, USA) developed the Polaris™ membrane, which is a TFC membrane in flat sheet format and packaged in spiral wound modules. A CO<sub>2</sub> permeance of 1000 GPU and a CO<sub>2</sub>/N<sub>2</sub> selectivity of 50 are reported,<sup>6</sup> with variations of this achieving 2000 and 4000 GPU with a concomitant selectivity decrease to 25 at the highest permeance.<sup>47</sup> Yave *et al.*<sup>48</sup> (GKSS Research Centre Geesthacht GmbH, Germany) reported TFC membranes derived from poly(ethylene oxide)-poly(butylene terephthalate) multiblock copolymer and the additive polyethylene glycol dibutyl ether. The dense film permeability was 750 Barrer with a CO<sub>2</sub>/N<sub>2</sub> selectivity of 40. TFCs prepared directly on a polyacrylonitrile support membrane yielded a CO<sub>2</sub> permeance of 510 GPU and a CO<sub>2</sub>/N<sub>2</sub> selectivity of 50. The incorporation of an additional polydimethylsiloxane gutter layer increased the permeance to 690 GPU, while the selectivity decreased to 40, matching the dense film value.

Of the multitude of polymeric membrane materials with high CO<sub>2</sub> permeability and adequate CO<sub>2</sub>/N<sub>2</sub> selectivity, only a small number have been conveyed into industrial practice as commercial membranes. In this perspective review, we highlight

five classes of highly permeable polymeric materials: polyimides, thermally rearranged polymers (TR polymers), substituted polyacetylenes, polymers of intrinsic microporosity (PIM) and poly(ethylene oxide) (PEO)-based polymers, because the majority of these polymers exhibit excellent characteristics for CO<sub>2</sub> separation applications (Fig. 1).

#### 3.1. High permeability polyimides

Polyimides are attractive materials for gas separation owing to their excellent gas separation and physical properties, such as high thermal stability, chemical tolerance, and mechanical strength.<sup>49</sup> They are commonly prepared by step polymerization involving a thermal or chemical imidization between a bis(carboxylic anhydride) and a diamine. The variation in structure–property relationships of polyimide membranes has been studied, relative to molar volume, density, free volume, and gas permeabilities by means of group contribution theory.<sup>50,51</sup> Generally, polymer chain rigidity determines the diffusivity–selectivity while inter-chain spacing and chain mobility govern the diffusion rate. The main factors affecting the gas transport properties in polyimide membranes are (1) spatial linkage configurations, (2) type of bridging groups, and (3) bulky and polar groups incorporated into the structures.<sup>52</sup>

In the molecular design of polyimides for gas separation of commercially important gas pairs such as CO<sub>2</sub>/CH<sub>4</sub>, previous research suggests that the selectivity in polyimide membranes can be enhanced by incorporating (1) *meta*-linkages, (2) swivel linkages comprising bulky groups, and (3) polar and bulky pendant groups.<sup>52</sup> For instance, asymmetric polyimides with *meta*-linkages show higher chain packing efficiency and restricted rotational freedom compared to the corresponding symmetric para-linked isomers.<sup>53,54</sup> As a result, the *meta*-isomers show moderately lower FFV and gas permeability, but higher gas selectivity. Also, polyimides with bulky bridging groups reduce inter-chain rotation, resulting in less chain mobility and higher FFV. For example, polyimides derived from 4,4'-(hexafluoroisopropylidene)diphthalic anhydride (6FDA) with diamines such as 2,3,5,6-tetramethyl-1,4-phenyldiamine (4MPDA)<sup>55,56</sup> and 3,3'-dimethylnaphthidine (DMN)<sup>57,58</sup> have increased chain stiffness due to the introduction of –C(CF<sub>3</sub>)<sub>2</sub>– linkages. This linkage is believed to serve as a molecular spacer and a chain stiffener; it reduces the intra-segmental mobility and limits the degree of chain packing thereby increasing the FFV. As a result, aromatic polyimides incorporating –C(CF<sub>3</sub>)<sub>2</sub>– linkages tend to have both high CO<sub>2</sub> permeability and high CO<sub>2</sub>/CH<sub>4</sub> selectivity.

The incorporation of spatial bridging groups into polyimides increases the free volume elements significantly. Polyimides containing spiro-centres,<sup>59–62</sup> bulky bis-phenylfluorenyl<sup>63</sup> and three-dimensional rigid triptycene frameworks<sup>64</sup> have been reported, which exhibit some of the highest permeability and selectivity data so far for polyimides, even exceeding the empirical upper bound performance limit. Polyimides with high free volume and appropriate cavity size to separate gas molecules of similar kinetic diameter, as well as those with polar or bulky groups, such as silica pendant groups,<sup>65</sup> hydroxyl, carboxylic acid, and sulfonic acids, or other bulky groups, were also reported.<sup>66</sup> The presence of bulky and polar pendant groups increases inter-chain spacing and reduces the packing efficiency

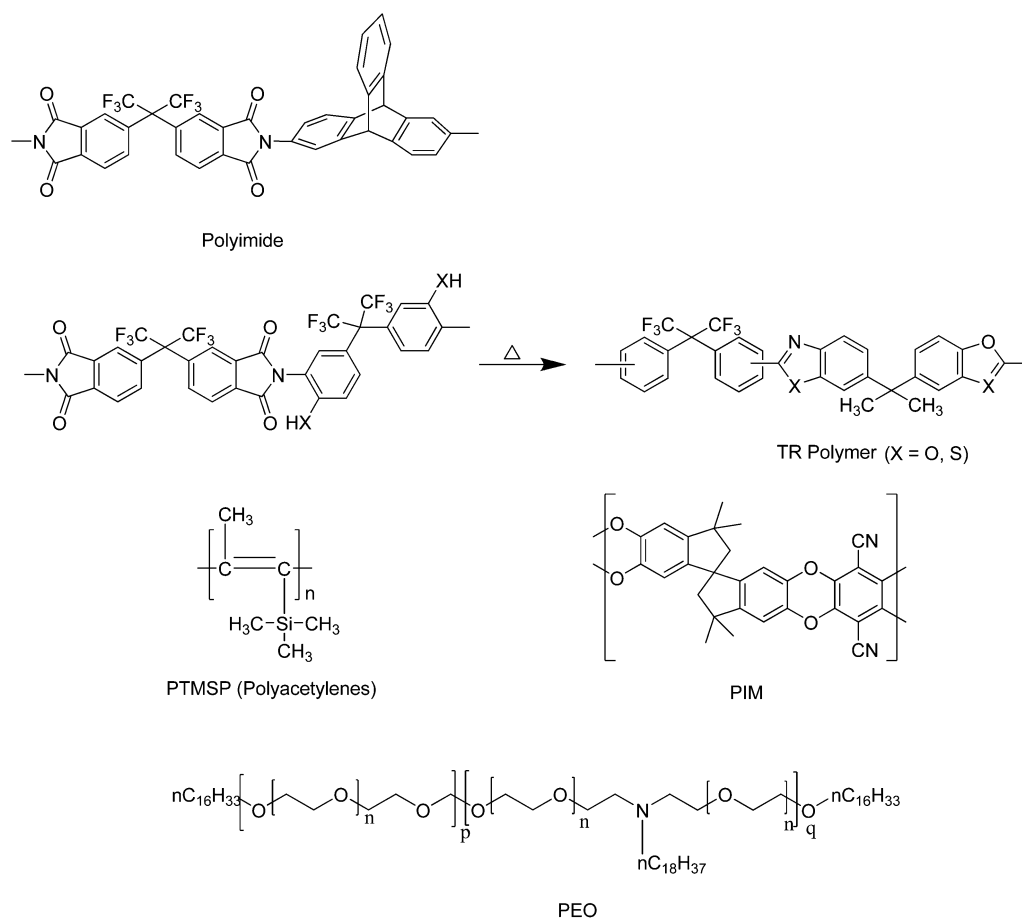


**Fig. 1** Representative chemical structures of polymers with high CO<sub>2</sub> permeability.

of polymer chains, hence significantly improving permeability. Furthermore, gas transport properties in polyimides are influenced by hydrogen bonding and intermolecular interactions.<sup>67,68</sup>

However, problems related to the swelling and plasticization of polyimides by CO<sub>2</sub> with mixed gases has hindered their adoption in CO<sub>2</sub> gas separation applications. In general, glassy polymers, including polyimides, swell by sorption of CO<sub>2</sub> that is present in a mixed gas, thereby increasing the permeation of other species (e.g., CH<sub>4</sub> and N<sub>2</sub>) in the mixed gas. Hence, the increased permeability of the 'slower' gas in the mixture results in losses in selectivity, in mixed gas separations. Since plasticization and physical aging originate from chain flexibility and the non-equilibrium state of glassy polymers, several approaches can mitigate these undesirable phenomena by increasing polymer chain rigidity or by inter-chain crosslinking. For example, plasticization-resistant membranes were prepared by cross-linking of carboxyl-containing polyimides with aliphatic diamines (C2–C4) or propanediol or by a thermal decarboxylation cross-linking reaction.<sup>69</sup> Cross-linking not only offers the potential to improve the mechanical and thermal properties of a membrane, but also improve gas transport properties. Polyimide networks in conjunction with pseudo-interpenetrating networks (IPNs) also restrict the mobility of the polymer chains and suppress CO<sub>2</sub>-induced plasticization.<sup>70</sup> In addition, polycondensation of dianhydride and tetraamine monomers provide polypyrrolones, which are structurally similar to polyimides. However, they have considerably more rigid chains due

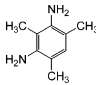
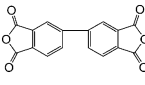
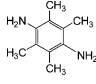
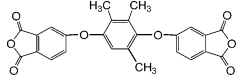
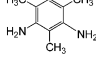
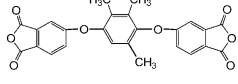
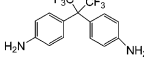
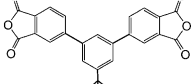
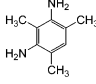
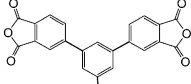
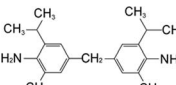
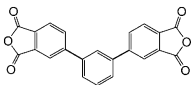
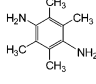
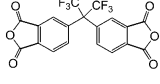
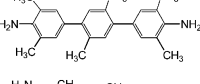
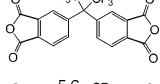
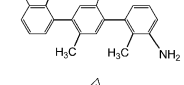
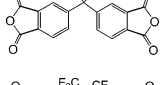
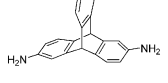
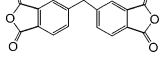
to the ladder structures, with higher thermal and chemical resistance, and behave in a manner analogous to organic molecular sieves.<sup>71–73</sup> Pure gas permeability and selectivity of highly permeable polyimide membranes are shown in Table 1.

More recently, a triptycene polyimide design was reported,<sup>64</sup> which has high internal free volume elements derived from three-dimensional rigid triptycene units, simultaneously having high permeability and selectivity. These triptycene polyimides are readily soluble in common organic solvents; thus they are processable for membrane fabrication. The triptycene-based polyimide exhibits very good tolerance to CO<sub>2</sub> plasticization in mixed gas separation,<sup>64</sup> e.g., CO<sub>2</sub>/CH<sub>4</sub>, while many glassy polymers having high FFV suffer from a large reduction in mixed gas selectivity. It is believed that this behavior arises from a physical hindrance effect due to the interlocking of the triptycene phenyl rings perpendicular to the polymer backbone, providing the spatial orientation for  $\pi$ – $\pi$  interactions to occur between phenyl rings. The triptycene-based polyimide membranes can impact emerging CO<sub>2</sub> gas separation applications such as natural gas purification and biogas purification for clean energy resources.

### 3.2. Thermally rearranged (TR) polymers

Membrane-based separation systems need to achieve both high gas throughput and high selectivity. For polymer membranes, separations depend on the size of the cavities that lead to

**Table 1** Gas permeability and selectivity in selected polyimide dense membranes<sup>64,74–77</sup>

Polyimide monomers		$\Delta P$	$T/^\circ\text{C}$	$P(\text{CO}_2)/$ Barrer	$P(\text{N}_2)/$ Barrer	$P(\text{CH}_4)/$ Barrer	$\alpha_{\text{CO}_2/\text{N}_2}$	$\alpha_{\text{CO}_2/\text{CH}_4}$	Ref.
Amine	Anhydride								
		10 atm	35	137	8.42	8.08	16.3	17	74
		1 atm	30	200	8.1	7.6	24.7	26.3	75
		1 atm	30	110	3.8	4.0	28.9	27.5	75
		3 atm	—	114	5.8	5.0	19.6	22.9	76
		3 atm	—	600	35.1	47.6	17.1	12.6	76
		3 atm	—	196	10.8	14.7	18.1	13.4	76
		10 atm	35	440	35.6	28.2	12.4	15.6	74
		1 atm	30	360	16.5	15.0	21.8	24.0	77
		1 atm	30	190	7.3	5.6	26.0	33.9	77
		1 atm	35	189	8.1	6.2	23.3	30.5	64

porosity on the sub-nanoscale. These cavities, so-called free volume elements, generally exhibit a broad scale distribution. Recently, rod-like polymers were derived from functionalized polyimides by a thermal post-membrane conversion process, *i.e.*, thermally rearranged (TR) polymers. These appear to have more uniform cavity sizes that create tailored free volume elements with well-connected morphology in amorphous polymers. The TR membranes have outstanding transport and separation properties for small gas molecules and ions. The TR membrane concept was proposed by Park *et al.* and Lee *et al.*,<sup>78,79</sup> which adopts a post-membrane fabrication polymer-modifying reaction to obtain dense polybenzoxazole (PBO) and polybenzothiazole (PBT) membranes by the thermal rearrangement of soluble aromatic polyimides containing ortho-linkage positioned functional groups (*e.g.*,  $-\text{OH}$  and  $-\text{SH}$ ). The TR polymers exhibit excellent separation performance, particularly for  $\text{CO}_2/\text{CH}_4$  mixtures, with high selectivity and

permeability due to an unusual microstructure whose cavity size and distribution could be further controlled by the appropriate selection of template molecules and heat treatment protocols. The unexpected physical phenomena in TR polymers are of great importance in that the random chain conformations occurring in the condensed polymer phase lead to tuned microvoids, which contribute to performance enhancement in selective molecular transport. A benefit of the thermal rearrangement concept is the relatively easy degree of control over the average interchain spacing and free volume elements that directly lead to molecular sieving effects. Thermal rearrangement is a feasible method for producing polymeric membranes with high permeability and selectivity suitable for gas separations.

One of the attractive features of TR membranes is their strong tolerance to plasticization in mixed-gas permeation experiments at  $35^\circ\text{C}$  for  $\text{CO}_2$  partial pressures<sup>78</sup> reaching 20 atm. The same

group reported a series of TR polymer membranes with ultrahigh gas selectivity derived from structurally different copolymer precursors, and hypothesized that the use of copolymers is desirable to generate desired polymeric properties to enable them to be processed into hollow fibre or flat sheet form.<sup>80</sup> The polymeric precursors are composed of polyimide (PI) and hydroxyl-containing polyimide (HPI), the latter of which can be thermally converted to TR polybenzoxazole (PBO) units. As a result, the surface area and pore volume varied significantly relative to the ratio of PBO to PI domains. Gas permeation and separation performance (*e.g.*, O<sub>2</sub>/N<sub>2</sub> and CO<sub>2</sub>/CH<sub>4</sub>) were linearly dependent on the ratio of PBO to PI, surpassing the empirical upper bounds of conventional polymeric membranes. In addition, poly(benzoxazole-*co*-pyrrolone) (PBO-*co*-PPL) copolymers having various compositions were prepared by thermal rearrangements from the respective polyimide precursors containing hydroxyl or amino groups.<sup>81</sup> These copolymers showed CO<sub>2</sub> permeabilities greater than their precursors, as well as higher gas selectivity than the individual PBO or PPL homopolymers. Indeed, thermally rearranged copolymers of rigid-chain and selective pyrrolones with highly permeable benzoxazoles having high free volume elements are a novel route to enhance gas selectivity without a significant loss in gas permeability. Using a similar concept, microporous polybenzimidazole (TR-PBI) membranes were reported by thermal rearrangement.<sup>82</sup> The membranes showed exceptionally high permeability to small gas molecules as well as excellent molecular sieving properties. In general, typically structured PBI membranes have very rigid, well-packed chains due to their strong intermolecular interactions, resulting in very low gas permeabilities, which are unsuitable for gas separation. However, alkaline hydrolysis of PPL followed by thermal rearrangement led to highly permeable TR-PBI membranes having microporous character (*i.e.*, high fractional free volume). A summary of data for selected TR polymers is shown in Table 2.

### 3.3. Highly permeable substituted polyacetylenes

Highly permeable substituted polyacetylenes generally have many molecular scale voids, which are formed by the presence of bulky pendant groups. They are prepared by polymerization of acetylenic monomers using transition metal catalysts.<sup>83</sup> It is known that various metal catalysts yield polymers with different geometric structures and properties. For example, NbCl<sub>5</sub> gives a more *cis*-rich poly(1-trimethylsilyl-1-propyne) (PTMSP) than TaCl<sub>5</sub>.<sup>84</sup> The pendant groups inhibit rotation of the rigid backbone,<sup>85</sup> which leads to inefficient chain packing (Table 3). The large free volume distribution includes both small disconnected elements and larger continuous microvoids. However, the large free volume elements collapse with time owing to vapour sorption, contamination<sup>86</sup> and/or relaxation phenomena, resulting in significant decreases in gas permeability.

PTMSP and related polymers in the class are among the most permeable polymers to any gases, having almost ten times higher permeability than the rubbery polymer poly(dimethylsiloxane). Hence, their gas transport properties have been extensively studied.<sup>87–89</sup> Although glassy PTMSP exhibits some properties that are similar to rubbers, gas transport through polyacetylenes is described in terms of the dual-mode sorption mechanism.<sup>90</sup>

The molecular design for highly permeable polyacetylenes has usually focused on incorporating different substituent groups. It has been deduced that the steric shape of the substituents attached to poly(diphenylacetylenes) plays a very important role in gas permeability.<sup>91,92</sup> Polyacetylenes with *tert*-butyl substituents provide higher permeability. In 2008, Hu *et al.* reported an indan-containing poly(diphenylacetylene) derivative, which exceeded the oxygen permeability of even PTMSP, which previously had the highest permeability.<sup>93</sup> In some substituted polyacetylenes, especially those with very high *P* values, which were based on both high diffusivity and solubility contributions, long-chain *n*-alkyl substituents gave relatively high diffusivity, while those with phenyl substituents had relatively high solubility.<sup>83</sup> It is believed that large microvoids give rise to high diffusion coefficients compared to other glassy polymers and also lead to high apparent solubility coefficients.

Although substituted polyacetylenes have characteristically high permeabilities, their selectivities are low, in accordance with performance trade-off behavior. Furthermore, significant aging problems in polyacetylenes impede their application in industrial membranes. Although polyacetylene-based membranes have high CO<sub>2</sub> permeability, they have not been considered for CO<sub>2</sub> separations because of low selectivity and strong physical aging. Nevertheless, there are opportunities for improving the properties of substituted polyacetylenes through macromolecular structural design. For example, approaches include grafting CO<sub>2</sub>-philic groups onto the PTMSP backbone, in order to enhance the solubility selectivity,<sup>94</sup> reversing aging by methanol treatment,<sup>95</sup> or reducing aging effects by cross-linking the membrane.<sup>96</sup>

### 3.4. Polymers with intrinsic microporosity

High free volume polymers can be achieved through rigid ladder backbone structures, instead of linear chains formed by single bonds with rotational freedom. Ladder polymers have traditionally been considered to be generally dense, intractable materials with poor mechanical properties. The basis for this is founded on the premise that linear ladder polymers are unable to form highly entangled chain matrices. However, in 2002, pioneering work on new ladder polymers incorporating ‘sites of contortion’ was reported by Budd and McKeown. Originally, the concept developed out of work aimed at producing high surface area cross-linked polymer networks incorporating catalytic centres.<sup>97,98</sup> Subsequently it was found that readily soluble, membrane-forming rigid ladder polymers with good mechanical properties could be prepared.<sup>99,100</sup> This class of materials is obtained by polycondensation reaction of tetrahydroxy-monomers containing spiro- or contorted centres with tetrafluoro-monomers.<sup>101,102</sup> The resulting ladder polymer backbones have no degrees of conformational freedom, but are sufficiently contorted to prevent effective packing in the solid state as well as to provide some mechanical strength through entanglement.<sup>103</sup> Furthermore, the microporous structures of these polymers are not as highly dependent on process and thermal treatment history as previous materials, and hence the term ‘polymers of intrinsic microporosity’ (PIM) was coined by the inventors. Compared with conventional molecular sieves, they represent a new class of microporous material with interconnected pores



**Table 2** Gas permeability and selectivity in selected TR dense membranes<sup>78–82</sup>

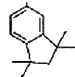
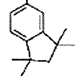
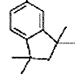
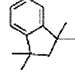
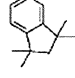
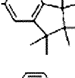
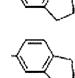
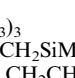
TR-polymer	Polymer precursors		$\Delta P$	$T/^\circ\text{C}$	$P(\text{CO}_2)/$ Barrer	$P(\text{N}_2)/$ Barrer	$P(\text{CH}_4)/$ Barrer	$\alpha_{\text{CO}_2/\text{N}_2}$	$\alpha_{\text{CO}_2/\text{CH}_4}$	Ref.
	Amine	Anhydride								
TRN	6FDA	DAB	1 atm	35	1624	62	35	26	46	82
TRS	6FDA	DABT	1 atm	35	1591	75	47	21	34	78 and 79
TRO-1	6FDA	bisAPAF	1 atm	35	1715	97	46	18	37	78 and 79
TRO-2	OPDA	bisAPAF	1 atm	35	73	2.2	1.3	33	58	78 and 79
TRO-3	BTDA	bisAPAF	1 atm	35	468	16	10	29	45	78 and 79
TRO-4	BPDA	bisAPAF	1 atm	35	629	20	16	32	41	78 and 79
TRO-5	PMDA	bisAPAF	1 atm	35	952	34	24	28	41	80
TRO-6	NTDA	bisAPAF	1 atm	35	4134	164	122	25	34	78 and 79
tPBO-1	6FDA	bisAPAF	1 atm	–	4201	284	151	15	28	81
aPBO-1	6FDA	bisAPAF	1 atm	–	398	19	12	21	34	81
cPBO-1	6FDA	bisAPAF	1 atm	–	5568	431	252	13	22	81
sPBO-1	6FDA	bisAPAF	1 atm	–	5903	350	260	17	23	81

less than 2 nm in size. Unlike inorganic microporous materials, such as zeolites and activated carbon, they generally have very good solubility and are thus readily processable.

The term ‘PIM-1’ was designated for a fluorescent yellow high molecular weight polymer with one of the simplest structures in the PIM class of materials, prepared by polycondensation reaction of commercial monomers 5,5,6,6-tetrahydroxy-3,3,3,3-tetramethylspiro-bisindane with tetrafluorophthalonitrile. PIM-1 is soluble in a number of solvents such as chloroform, toluene or

tetrahydrofuran, and can be cast from solution to form robust membranes. Low-temperature N<sub>2</sub> adsorption–desorption analysis indicates that PIM-1 in powder or membrane form has a high apparent surface area ( $S_{\text{BET}} = \sim 800 \text{ m}^2 \text{ g}^{-1}$ ) and exhibits microporous character. PIMs are considered as amorphous materials, since there is no evidence of crystallinity or a glass transition below the decomposition temperature. The latter observation may be expected, since there is no degree of chain rotational mobility, at least over short length scales. Initial data

**Table 3** Side groups and gas permeability and selectivity in selected substituted polyacetylene dense membranes at 25 °C<sup>38,93</sup>

(-CR=CR'-) <sub>x</sub>									
<i>R</i>	<i>R'</i>	<i>P</i> up/down	<i>P</i> (CO <sub>2</sub> )/Barrer	<i>P</i> (N <sub>2</sub> )/Barrer	<i>P</i> (CH <sub>4</sub> )/Barrer	α CO <sub>2</sub> /N <sub>2</sub>	α CO <sub>2</sub> /CH <sub>4</sub>	Ref.	
Me	SiMe <sub>3</sub>	1 atm/0.3 Pa	47000	11500	29900	4.09	1.57	93	
C <sub>6</sub> H <sub>4</sub> F ( <i>p</i> )		1 atm/0.3 Pa	47000	15600	34300	3.01	1.37	93	
C <sub>6</sub> H <sub>4</sub> F ( <i>m</i> )		1 atm/0.3 Pa	35200	12000	27800	2.93	1.26	93	
C <sub>6</sub> H <sub>3</sub> F <sub>2</sub> ( <i>p, m</i> )		1 atm/0.3 Pa	44200	16600	35000	2.66	1.26	93	
C <sub>6</sub> H <sub>3</sub> F <sub>2</sub> ( <i>m, m</i> )		1 atm/0.3 Pa	36100	13100	29100	2.76	1.24	93	
C <sub>6</sub> H <sub>4</sub> Me ( <i>p</i> )		1 atm/0.3 Pa	16900	4100	10100	4.12	1.67	93	
C <sub>6</sub> H <sub>5</sub>		1 atm/0.3 Pa	36400	10400	25200	3.50	1.44	93	
C <sub>6</sub> H <sub>4</sub> SiMe <sub>3</sub> ( <i>p</i> )		1 atm/0.3 Pa	2000	170	470	11.7	4.25	93	
C <sub>6</sub> H <sub>5</sub>		1 atm/0.3 Pa	390	30	60	13.0	6.50	93	
H	C(CH <sub>3</sub> ) <sub>3</sub>	1 atm/13 Pa	560	43	85	13.0	6.59	38	
Me	SiMe <sub>2</sub> CH <sub>2</sub> SiMe <sub>3</sub>	1 atm/13 Pa	310	21	45	14.8	6.89	38	
Me	SiMe <sub>2</sub> CH <sub>2</sub> CH <sub>2</sub> SiMe <sub>3</sub>	1 atm/13 Pa	150	14	28	10.7	5.36	38	
H	<i>o</i> -C <sub>6</sub> H <sub>4</sub> SiMe <sub>3</sub>	1 atm/13 Pa	290	24	38	12.1	7.64	38	
H	<i>o</i> -C <sub>6</sub> H <sub>4</sub> CF <sub>3</sub>	1 atm/13 Pa	130	7.3	6.6	17.8	19.7	38	
Me	<i>n</i> -C <sub>7</sub> H <sub>15</sub>	1 atm/13 Pa	130	14	40	9.29	3.25	38	
Cl	<i>n</i> -C <sub>8</sub> H <sub>17</sub>	1 atm/13 Pa	170	16	46	10.6	3.70	38	
Cl	<i>n</i> -C <sub>6</sub> H <sub>13</sub>	1 atm/13 Pa	130	11	33	11.8	3.94	38	
Cl	<i>n</i> -C <sub>4</sub> H <sub>9</sub>	1 atm/13 Pa	180	10	30	18.0	6.00	38	
H	CH( <i>n</i> -C <sub>5</sub> H <sub>11</sub> )SiMe <sub>3</sub>	1 atm/13 Pa	120	8.7	21	13.8	5.71	38	

for PIM-1 membranes exhibited gas permeabilities exceeded only by very high free volume polymers such as PTMSP and Teflon AF2400. Combined with selectivities, the performance trade-off is typically located between the 1991 and the 2008 Robeson upper bounds for gas pairs, such as O<sub>2</sub>/N<sub>2</sub> and CO<sub>2</sub>/CH<sub>4</sub> and it is an upper bound material for CO<sub>2</sub>/N<sub>2</sub>.<sup>104</sup> In the majority of glassy polymers, the typical order of permeability is He > CO<sub>2</sub>. However, PIM-1 has an unusually high CO<sub>2</sub> permeability, with the order of decreasing permeability being CO<sub>2</sub> > H<sub>2</sub> > He > O<sub>2</sub> > CH<sub>4</sub> > N<sub>2</sub>. This is because CO<sub>2</sub> selectivity for PIM-1 is dominated by solubility selectivity, and less so by diffusivity selectivity. Subsequent studies showed that permeability could be substantially enhanced by methanol treatment, Table 4, which helps to remove residual bound casting solvent.<sup>105</sup>

Although many PIMs could be theoretically prepared by double aromatic nucleophilic substitution (S<sub>N</sub>Ar) polycondensation, only a few PIM structures having high molecular weight have been reported. This can be attributed to (1) a limited choice of available monomers, (2) reactivity of available monomers in producing sufficiently high molecular weight polymers,

(3) poor solubility of the growing chain during polycondensation and (4) side reactions and cross-linking. Solvent processable materials with high molecular weight are crucial for fabricating gas separation membranes in the form of thin film composites, free-standing asymmetric membranes, or isotropic films.<sup>106</sup> Therefore, an important step in the evolution of PIMs for CO<sub>2</sub> selective separations is to expand the spectrum of high molecular weight materials having new structures, derived either from alternative monomers or by modification of the PIM polymer, for the purpose of determining the structure–gas transport properties of this unique class of materials. From the solution–diffusion model, an improvement in CO<sub>2</sub> permselectivity can be achieved by a combination of greater gas diffusivity selectivity or by an increase in the solubility of the faster gas (*i.e.* CO<sub>2</sub>) in the polymer matrix.

In the majority of previous work, increased performance was achieved mainly by improving diffusivity–selectivity through an increase in the chain rigidity or by tuning the cavity size. Three factors significantly affecting PIM diffusivity–selectivity appear to be (1) the molecular length of the quasi-linear ladder units

**Table 4** Gas permeability and selectivity in selected PIM dense membranes<sup>60,99,103,105–107,109,111,115–120</sup>

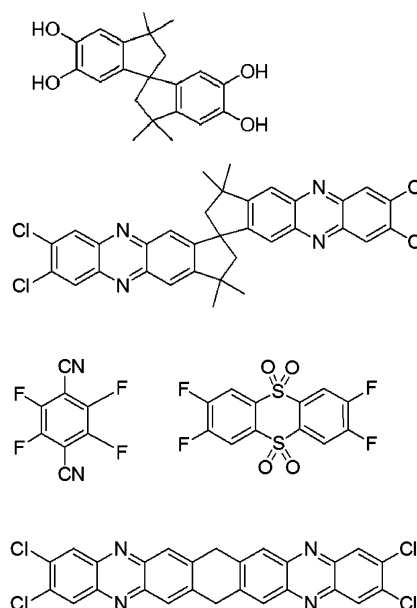
Polymeric membrane	$\Delta P$	$T/^\circ\text{C}$	$P(\text{CO}_2)/$ Barrer	$P(\text{N}_2)/$ Barrer	$P(\text{CH}_4)/$ Barrer	$\alpha_{\text{CO}_2/\text{N}_2}$	$\alpha_{\text{CO}_2/\text{CH}_4}$	Ref.
PIM-1 (methanol treated)	200–300 mbar	30 °C	11200	610	1160	18.4	9.6	105
PIM-1	200–300 mbar	30 °C	2300	92	125	25	18	120
PIM-7	200–300 mbar	30 °C	1100	42	62	26.2	17.7	103 and 120
TFMPSPIM1	3.4 atm	25 °C	731	33		22		116
DSPIM1-33	3.4 atm	25 °C	1408	88		16		106
DSPIM2-33	3.4 atm	25 °C	1077	52		20.7		106
DSPIM3-33	3.4 atm	25 °C	2154	93		23		106
DNPIIM-50	3.4 atm	25 °C	2627	132		19.9		111
TOTPIIM-100	3.4 atm	25 °C	3056	190		16.1		107
DNTOTPIIM-50	3.4 atm	25 °C	3065	172		18.0		107
C-PIM-1h	3.4 atm	25 °C	2543	162		15.7		115
C-PIM-2h	3.4 atm	25 °C	2058	99		20.8		115
C-PIM-3h	3.4 atm	25 °C	1056	48		22.0		115
C-PIM-4h	3.4 atm	25 °C	620	24		25.8		115
Cross-linked PIM-1/azide1 (80 : 20)	3.4 atm	25 °C	580	32		18.1		119
Cross-linked PIM-1/azide2 (80 : 20)	3.4 atm	25 °C	219	8		27.4		119
TZPIM-2	3.4 atm	25 °C	3076	101		30.5		118
TZPIM-1	3.4 atm	25 °C	2509	87		28.9		118
PIM-PI-1	200–300 mbar	30 °C	1100	48	77	22.9	14.3	60
PIM-PI-2	200–300 mbar	30 °C	210	9	9	23.3	23.3	60
PIM-PI-3	200–300 mbar	30 °C	520	23	27	22.6	19.3	60
PIM-PI-4	200–300 mbar	30 °C	420	16	20	26.3	21	60
PIM-PI-7	200–300 mbar	30 °C	510	19	27	26.8	18.9	60
PIM-PI-8	200–300 mbar	30 °C	3700	161	260	23.0	14.2	60
Cardo-PIM-1	200–300 mbar	30 °C	430	13	22	33	19.5	109
PIM-CO15	200–300 mbar	30 °C	2000	83	130	24.1	15.4	117
PIM1-CO15-75	200–300 mbar	30 °C	2570	110	180	23.4	14.3	117
PIM1-CO15-50	200–300 mbar	30 °C	4600	210	370	21.9	12.4	117
PIMCO1-CO15-50	200–300 mbar	30 °C	5400	240	350	22.5	14.3	117
PIMCO2-CO15-50	200–300 mbar	30 °C	5300	260	430	20.4	12.3	117
PIMCO6-CO15-50	200–300 mbar	30 °C	3800	170	280	22.4	13.6	117
PIMCO19-CO15-50	200–300 mbar	30 °C	3400	150	260	22.7	13.1	117
PIM-CO19	200–300 mbar	30 °C	6100	320	580	19.1	10.52	117

between contorted centres (Fig. 2), (2) the angle of the spiro- or contorted (twist) centres (Fig. 3), and (3) pendant groups on the polymer backbone (Fig. 4).

Pure gas permeability and selectivity of a variety of structural PIM membranes are shown in Table 4. The permeability/selectivity properties could be tuned by incorporating molecular units of different lengths between the spirocentres, such as thianthrene,<sup>107</sup> 9,10-dimethyl-9,10-dihydro-9,10-ethanoanthracene,<sup>108</sup> ethanoanthracene<sup>109</sup> and PIM-7 containing pyrazine.<sup>110</sup> The angle of the spiro or twist centres also affects the permeability/selectivity properties,<sup>111–114</sup> for example, dinaphthyl,<sup>111</sup> spiro-fused fluorene-based monomers,<sup>112</sup> and 1,2- or 1,4-di(3',4'-dihydroxyphenyl)tetraphenylbenzene.<sup>114</sup> Pendant substituents on the PIM backbone may also increase chain rigidity, and act as interchain filling material, which effectively tunes the cavity shape and size, such as carboxylic acid groups,<sup>115</sup> sulfone-based groups,<sup>106</sup> and trifluoromethyl groups.<sup>116</sup>

A different approach to enhancing CO<sub>2</sub> permselectivity is by increasing the solubility–selectivity of the “faster gas”, since even modest increases in solubility–selectivity should lead to obvious improvements in overall selectivity. Fritsch *et al.* reported novel PIMs with spiro-bischromane structures, one of which, PIMCO1-CO15-50 (Fig. 5), showed remarkably high solubility coefficients for CO<sub>2</sub> compared with PIM-1. Hence, although they may not provide a significant improvement over PIM-1 for separations involving permanent gases, this polymer has good

selectivity for separations involving condensable gases and vapors due to the enhanced solubility contribution to their overall permeability.<sup>117</sup>

**Fig. 2** PIM monomers providing different unit lengths.

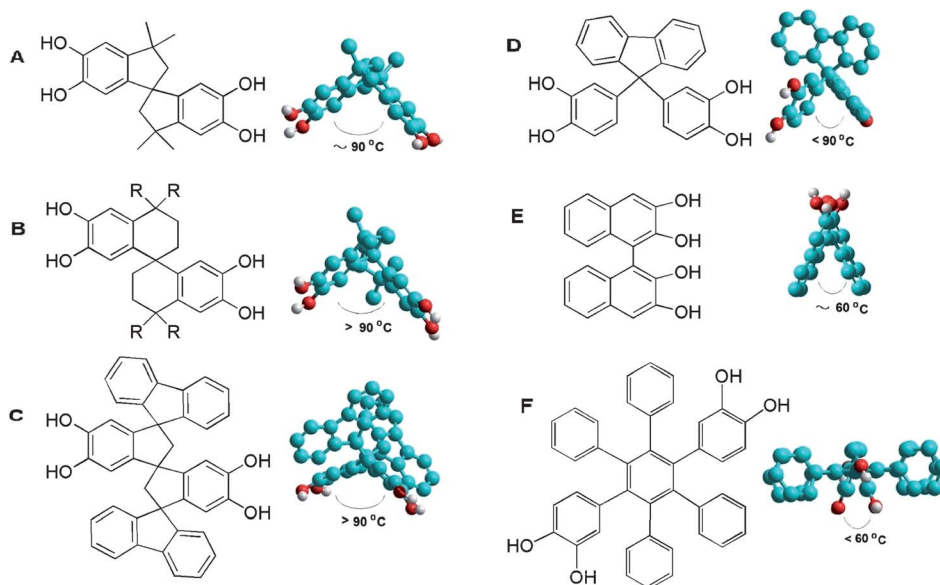


**Fig. 3** Visual models of PIM monomers with different angles of spiro or twist centres as simulated with energy minimization.

Recently, a new class of PIMs, incorporating tetrazoles (TZPIM, Fig. 5) into the microporous polymeric framework, was shown to have very high permeability for CO<sub>2</sub> and excellent CO<sub>2</sub>/N<sub>2</sub> mixed gas separation, even under polymer plasticization conditions (Fig. 6).<sup>118</sup>

The presence of the tetrazole groups leads to favorable CO<sub>2</sub> sorption and selective pore blocking by presorbed CO<sub>2</sub> molecules, thus limiting access by other light gas molecules such as nitrogen (Fig. 7). The introduction of tetrazoles into

PIM is the first example of a [2 + 3] cycloaddition modification of a polymer containing aromatic nitrile groups with an azide. This strategy of incorporating nitrogen heterocycles into PIMs provides new directions in the design of other polymeric membrane materials for important CO<sub>2</sub> separation processes.

PIMs also undergo some degree of physical aging and plasticization. PIM-1 was cross-linked with diazides in order to reduce plasticization at high CO<sub>2</sub> partial pressures.<sup>119</sup>

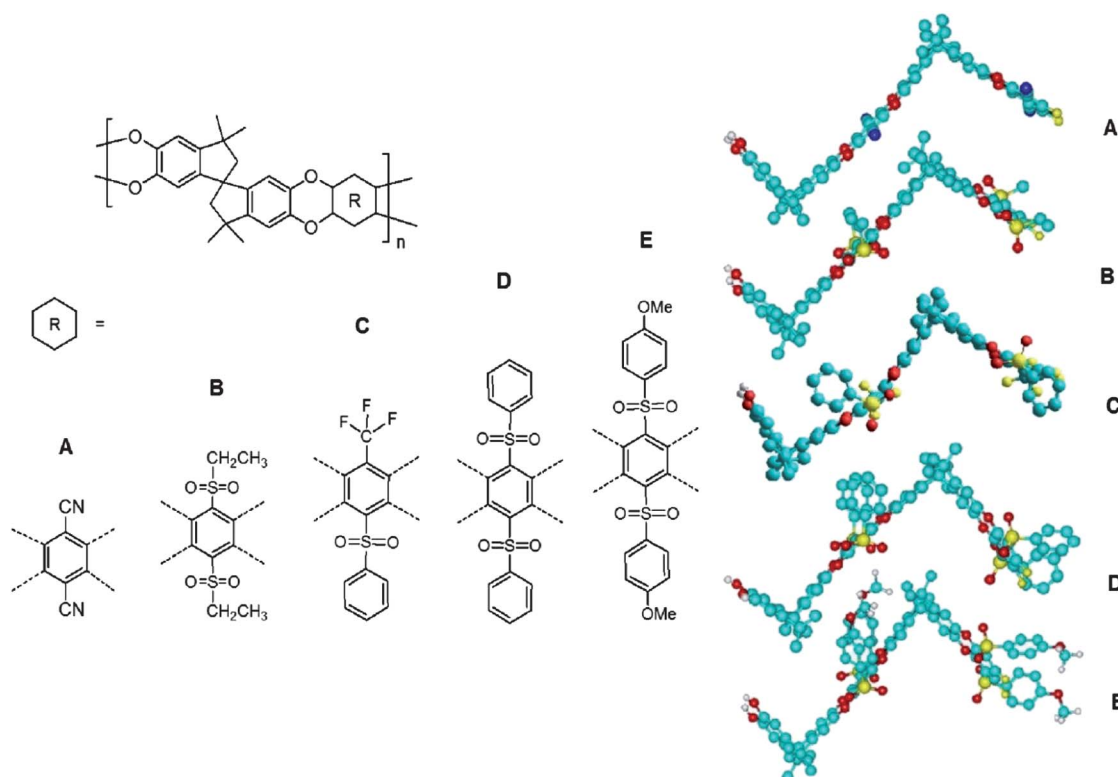


**Fig. 4** Visual models of PIM monomers with different pendent groups as simulated with energy minimization. Adapted from ref. 106 and 116.



### 3.5. Solubility-selective poly(ethylene oxide) (PEO) based membranes

PEO and PEG (poly(ethylene glycol)), or more generally, polyethers have been identified as outstanding CO<sub>2</sub>-selective materials, due to their relatively easy fabrication<sup>121,122</sup> and high performance, which has been attributed to the strong interaction between the high concentration of polar ether oxygen atoms and CO<sub>2</sub>.<sup>123</sup> However, PEO has a strong tendency to crystallize, due to the polar oxygen atoms in the matrix, bringing about efficient polymer chain packing that leads to significant reductions in gas permeability. There has been no systematic study of gas transport properties in pure PEO. Various strategies have been

proposed to inhibit or depress crystallization by changing the content and molecular weight of the ethylene oxide segment or by tuning of the micro-domain morphology. Among the main techniques to reduce crystallinity in PEO, the design of purely polymer structures, such as block copolymers with short ethylene oxide (EO) segments that effectively prevent crystallization at room temperature, and highly branched, cross-linked PEO networks, has attracted the most attention.

The copolymers typically have microphase-separated structures containing soft PEO segments and hard segments such as polyamides,<sup>126</sup> (Pebax® polyether block amide), polyimides<sup>127</sup> and polysulfone.<sup>128</sup> The hard segments provide mechanical stability and inhibit crystallization of PEO. The PEO phase in

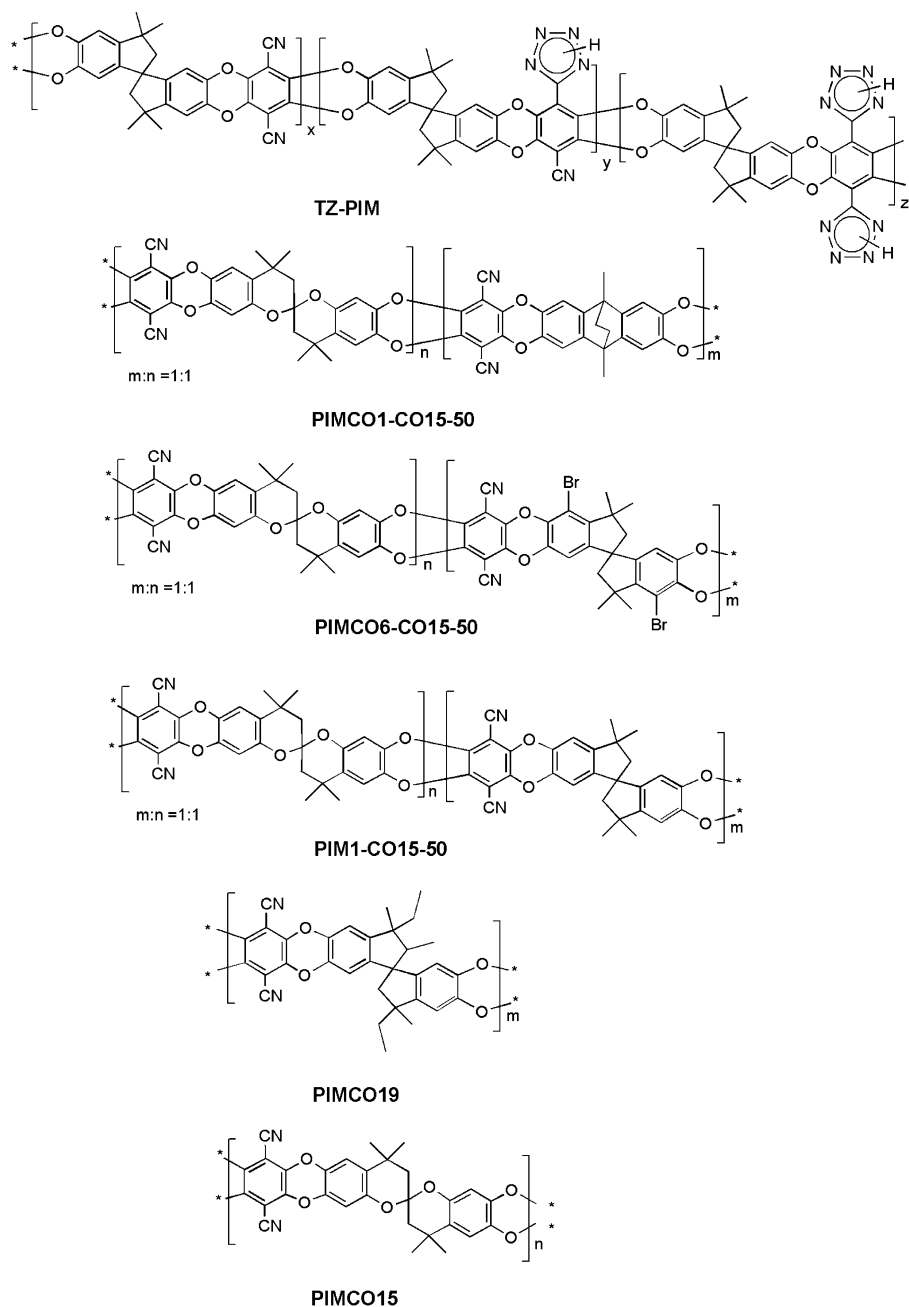
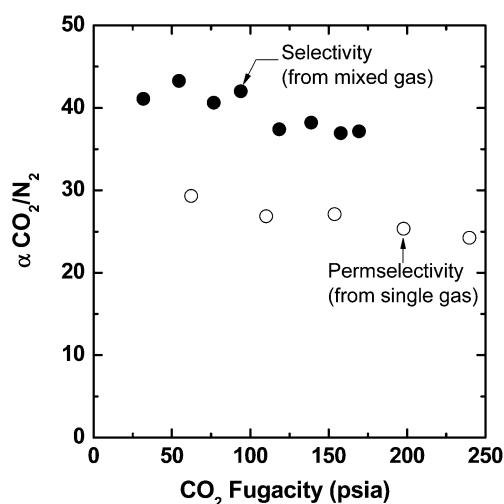


Fig. 5 PIMs with high solubility coefficients.<sup>117,118</sup>

these block copolymers is believed to be the continuous pathway for gas diffusion, because the  $\text{CO}_2/\text{N}_2$  selectivity in these copolymers is similar to pure PEO. The morphology is believed to determine the gas permeability *via* the domain shape and spatial arrangement, which is influenced by the hard segment composition and the lengths of the PEO and hard segment blocks. The development of innovative PEO membranes, which are capable of efficiently and selectively permeating  $\text{CO}_2$  from other gases while maintaining high permeability, though challenging, has been successfully achieved with the Polaris™ membrane from MTR<sup>6</sup> and the PEO–PBT + PEG–DBE from GKSS.<sup>48</sup>

Several PEO copolymers with high  $\text{CO}_2$  permeability are reported (Table 5). Recently, Nijmeijer *et al.*<sup>129,130</sup> reported a series of PEO membranes based on a highly permeable polyether-based segmented block copolymer. For example, a block copolymer system based on soft segments containing a random distribution of PEO and PPO and uniform tetra-amide (T6T6T) hard segments, referred to as PEO-*ran*-PPO-T6T6T, achieved  $\text{CO}_2$  permeabilities as high as 470 Barrer with a selectivity of 43 for the  $\text{CO}_2/\text{N}_2$  gas pair.<sup>131</sup> The PEO copolymer was further modified to give significantly higher  $\text{CO}_2$  permeability and  $\text{CO}_2$ /light gas selectivity by introducing certain additives. When PEO-*ran*-PPO<sub>5000</sub>-T6T6T was blended with poly[dimethylsiloxane-*co*-methyl(3-hydroxypropyl)siloxane]-graft-poly(ethylene glycol)methyl ether–PDMS–PEG,  $\text{CO}_2$  permeability of blends increased from 447 to 896 Barrer with a selectivity decrease from 42.5 to 36.0 for the  $\text{CO}_2/\text{N}_2$  gas pair.<sup>132</sup> Further development of highly permeable block copolymer systems for  $\text{CO}_2$  separation based on the concept of combining soft and hard segments in PEO-based membranes is an active area of research.

Cross-linked polymers based on PEO, having less crystallinity, have been prepared by plasma irradiation<sup>133</sup> or UV photopolymerization.<sup>134</sup> These materials may provide improved



**Fig. 7** Effect of  $\text{CO}_2$  partial pressure on mixed-gas  $\text{CO}_2/\text{N}_2$  selectivity in TZPIM-2 at 25 °C. Mixed gas composition (in mol%  $\text{CO}_2$ : mol%  $\text{N}_2$ ) was 50 : 50. Adapted from ref. 118. Nature Publishing Group, Macmillan Publishers Ltd.

chemical resistance and suppressed plasticization by  $\text{CO}_2$  (or other gas impurities). Hirayama<sup>135</sup> increased the  $\text{CO}_2$  permeability of pure PEG dimethacrylate (DM) from 45 Barrer to 210 Barrer by increasing the content of PEG methyl ether methacrylate. Similarly, the  $\text{CO}_2$  permeability of 2,2-bis(4-methacryloxy polyethoxy phenyl)propane (DB) was increased from 93 to 250 Barrer in the same manner. The  $\text{CO}_2/\text{N}_2$  selectivity generally decreased from 69 to 60 at 25 °C with increasing permeability. Lin *et al.*<sup>122,124,133</sup> reported cross-linked PEO diacrylate (PEGDa) films with  $\text{CO}_2$  permeability increasing from 110 to 570 Barrer as the PEG methyl ether acrylate (PEGMEA) content was

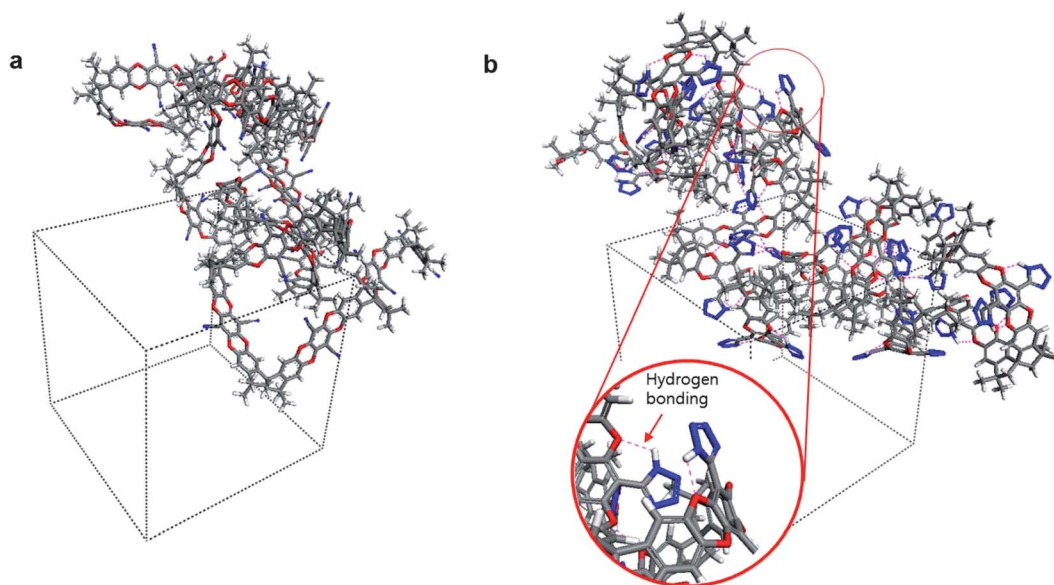


**Fig. 6** (a) Three-dimensional view of PIM-1 in an amorphous periodic cell (the number of repeat units in PIM-1 is 20), and (b) a three dimensional view of TZPIM-3 containing tetrazole in an amorphous periodic cell (the number of repeat units in TZPIM is 20; 100% full conversion from nitrile groups to tetrazole groups; the blue dotted lines indicate possible hydrogen bonding modes). Adapted from ref. 118. Nature Publishing Group, Macmillan Publishers Ltd.

**Table 5** Pure gas CO<sub>2</sub> permeability and CO<sub>2</sub>/N<sub>2</sub> selectivity in selected PEO containing polymers<sup>48,124–126,135</sup>

Polymer type	Membrane designation <sup>b</sup>	$\Delta P$	Temperature	$P(\text{CO}_2)^a/\text{Barrer}$	$\alpha \text{ CO}_2/\text{N}_2$	Ref.	
Block copolymer	P6: PMDA-APPS/PEO3(80)	2 atm	35 °C	159	51	125	
	P7: PMDA-APPS/PEO4(70)	2 atm	35 °C	136	53	125	
	P8: PMDA-mPD/PEO(80)	2 atm	35 °C	151	52	125	
	P9: PMDA-ODA/PEO4(80)	2 atm	35 °C	167	52	125	
	P10: PMDA-pDDS/PEO4(80)	2 atm	35 °C	238	49	125	
	B14: BPDA-ODA/PEO4(80)	2 atm	35 °C	117	51	125	
	55PEO/PA6	10 atm	35 °C	120	52	126	
	Block copolymer crosslinked poly (ethylene oxide)	PEGDA/PEGMEA(0)	4 atm	35 °C	112	52	124
		PEGDA/PEGMEA(20)	4 atm	35 °C	150	58	124
		PEGDA/PEGMEA(50)	4 atm	35 °C	250	41	124
PEGDA/PEGMEA(70)		4 atm	35 °C	320	47	124	
PEGDA/PEGMEA(91)		4 atm	35 °C	520	41	124	
PEGDA/PEGMEA(99)		4 atm	35 °C	570	41	124	
DM14/MM9(30)		1 atm	35 °C	129	51	135	
DM14/MM9(50)		1 atm	35 °C	185	50	135	
DM14/MM9(70)		1 atm	35 °C	260	48	135	
DB30/MM9(0)		1 atm	35 °C	128	49	135	
DB30/MM9(10)		1 atm	35 °C	140	50	135	
DB30/MM9(30)		1 atm	35 °C	185	51	135	
DB30/MM9(50)		1 atm	35 °C	231	48	135	
DB30/MM9(70)		1 atm	35 °C	308	47	135	
DM23/MM9(10)		1 atm	35 °C	194	52	135	
PEO–poly(butylene terephthalate)		PEO–PBT	0.3 atm	30 °C	150	52	48
		PEO–PBT + PEG	0.3 atm	30 °C	208	49	48
		PEO–PBT + PEG–BE	0.3 atm	30 °C	400	50	48
		PEO–PBT + PEG–DBE	0.3 atm	30 °C	750	40	48

<sup>a</sup> CO<sub>2</sub> permeabilities for ref. 135 are predicted values at 35 °C by interpolation of an Arrhenius plot and the CO<sub>2</sub>/N<sub>2</sub> selectivity is the ratio thereof. The data are restricted to  $P(\text{CO}_2) > 100$  Barrer. <sup>b</sup> The numbers in parentheses refer to the mass fraction of the second component.

increased from zero to 99%. The CO<sub>2</sub>/N<sub>2</sub> selectivity decreased from 58 to 41 at 35 °C, which is comparable to the selectivity range observed by Hirayama when corrected to the same temperature (Table 5).

#### 4. Conclusions

Membrane technology could play an important role in separating or capturing CO<sub>2</sub> from large point sources such as coal-fired power plants, cement and steel plants. Membranes compete with other separation processes on the basis of overall economics, safety, environmental and technical aspects. Thus, improving the separation performance of polymeric membranes for CO<sub>2</sub> capture from flue gas and other industrial sources is a very active area of research. In this perspective review, five different classes of polymers have been discussed as high permeability materials for gas separation membranes that are effective for separating CO<sub>2</sub>. Useful CO<sub>2</sub> separation membranes should ideally possess a number of properties such as (1) high CO<sub>2</sub> permeability (more practically, high CO<sub>2</sub> flux), (2) high CO<sub>2</sub>/gas selectivity (especially mixed gas selectivity, rather than pure gas permselectivity), (3) tolerance against CO<sub>2</sub> plasticization, (4) no severe physical aging, (5) low cost, (6) ability to be economically fabricated into different membrane modules (*e.g.*, hollow fibre or spiral wound modules) and (7) thermal and chemical resistance.

Polyimides are well-known materials for gas separations, because of their gas separation properties, high thermal stability, chemical tolerance, and mechanical strength. Although some polyimides are susceptible to swelling and plasticization by CO<sub>2</sub>

with mixed gases, resulting in reduced selectivity, several approaches such as increasing polymer chain rigidity and inter-chain cross-linking can mitigate these undesirable phenomena. Polyacetylenes generally have extremely high CO<sub>2</sub> permeability, but selectivities are very low. By substitution of certain pendent groups on the chain, selectivities can be increased significantly, with the expected declines in permeability. Polyacetylenes also suffer from rapid physical aging, leading to significant declines in permeability. PEOs are highly selective and permeability can be increased by several methods, such as cross-linking, bulky end groups, and copolymers, to create crystalline/non-crystalline domains. Furthermore, PEO-based materials are the one class of polymer materials that have been transformed into working membranes. The direction of research for CO<sub>2</sub>-selective polymer membrane materials in recent years is to achieve ultra-high CO<sub>2</sub> permeability in polymers *via* new concepts—cavity engineering in rigid or semi-rigid, amorphous glassy polymers for improving both fast CO<sub>2</sub> diffusion and CO<sub>2</sub> sorption capacity. PIMs and TR polymers are representative polymers belonging to this family. These polymers have rigid backbones, retaining high selectivity, and the free volume elements (cavity sizes and shapes) can also be further controlled *via* physical and chemical modification methods, which lead to high diffusion rates through cavities. Subtle changes in molecular architecture can result in profound effects on gas permeation and separation properties. That is, the diffusivity–selectivity can be enhanced by increasing free volume and tuning its distribution. The solubility can be enhanced by introducing CO<sub>2</sub>-philic groups. Additionally, it is also important to ensure that membranes are physically durable and resistant to both chemical attack and plasticization, while

maintaining good processability. For this reason, research efforts must be directed towards designing readily processable polymers that have desirable combinations of permeability and selectivity, with long-term stability, in order to have immediate significant impact on scale-up and commercialization.

## Acknowledgements

NRC publication number 53042. The research support from the Clean Energy Fund, Energy Sector, Office of Energy R&D, Natural Resources Canada (NRCan) is gratefully acknowledged by ND, MDC and MDG. The research support from the WCU (World Class University) program, National Research Foundation (NRF) of the Korean Ministry of Science and Technology (no. R31-2008-000-10092-0), is gratefully acknowledged by HBP and MDG.

## References

- 1 IPCC Special Report on Carbon Dioxide Capture and Storage, ed. B. Metz, O. Davidson, H. C. de Coninck, M. Loos and L. A. Meyer, Cambridge University Press, Cambridge, England, 2005.
- 2 IPCC Third Assessment Report: Climate Change 2001, Cambridge University Press, Cambridge, England, 2001.
- 3 P. Friedlingstein, R. A. Houghton, G. Marland, J. Hackler, T. A. Boden, T. J. Conway, J. G. Canadell, M. R. Raupach, P. Ciais and C. Le Quéré, *Nat. Geosci.*, 2010, **3**, 811–812.
- 4 N. MacDowell, N. Florin, A. Buchard, J. Hallett, A. Galindo, G. Jackson, C. S. Adjiman, C. K. Williams, N. Shah and P. Fennell, *Energy Environ. Sci.*, 2010, **3**, 1645–1669.
- 5 J. D. Figueroa, T. Fout, S. Plasynski, H. McIlvried and R. D. Srivastava, *Int. J. Greenhouse Gas Control*, 2008, **2**, 9–20.
- 6 T. C. Merkel, H. Lin, X. Wei and R. Baker, *J. Membr. Sci.*, 2010, **359**, 126–139.
- 7 E. Favre, *J. Membr. Sci.*, 2007, **294**, 50–59.
- 8 T. Graham, *Philos. Mag.*, 1866, **32**, 401–420.
- 9 S. Loeb and S. Sourirajan, *US pat.*, 3133132, 1964.
- 10 C. A. Scholes, S. E. Kentish and G. W. Stevens, *Recent Pat. Chem. Eng.*, 2008, **1**, 52–66.
- 11 R. W. Baker, W. Koros, E. L. Cussler, R. L. Riley, W. Eykamp and H. Strathmann, Gas Separation, in *Membrane Separation Systems—Recent Developments and Future Directions*, Noyes Data Corporation Press, 1991, p. 199.
- 12 W. Mazur and M. Chan, *Chem. Eng. Prog.*, 1982, **78**, 38–43.
- 13 A. Coady and J. Davis, *Chem. Eng. Prog.*, 1982, **78**, 43–49.
- 14 P. M. Budd and N. B. McKeown, *Polym. Chem.*, 2010, **1**, 63–68.
- 15 M. Czyperek, P. Zapp, H. J. M. Bouwmeester, M. Modigell, K. Ebert, I. Voigt, W. A. Meulenber, L. Singheiser and D. Stover, *J. Membr. Sci.*, 2010, **359**, 149–159.
- 16 E. R. Watson, G. V. Rowley and C. R. Wunderlich, *US pat.*, 3432585, 1969.
- 17 H. Lin and B. D. Freeman, *J. Mol. Struct.*, 2005, **739**, 57–74.
- 18 C. E. Powell and G. G. Qiao, *J. Membr. Sci.*, 2006, **279**, 1–49.
- 19 A. Brunetti, F. Scura, G. Barbieri and E. Drioli, *J. Membr. Sci.*, 2010, **359**, 115–125.
- 20 L. M. Robeson, *J. Membr. Sci.*, 1991, **62**, 165–185.
- 21 L. M. Robeson, *J. Membr. Sci.*, 2008, **320**, 390–400.
- 22 D. Lee and S. T. Oyama, *J. Membr. Sci.*, 2002, **210**, 291–306.
- 23 D. W. Breck, *Zeolite Molecular Sieves*, Wiley-Interscience, New York, 1974.
- 24 W. J. Koros, G. K. Fleming, S. M. Jordan, T. H. Kim and H. H. Hoehn, *Prog. Polym. Sci.*, 1988, **13**, 339–401.
- 25 M. M. Dal-Cin, A. Kumar and L. Layton, *J. Membr. Sci.*, 2008, **323**, 299–308.
- 26 L. M. Robeson, B. D. Freeman, D. R. Paul and B. W. Rowe, *J. Membr. Sci.*, 2009, **341**, 178–185.
- 27 *Polymeric Gas Separation Membranes*, ed. D. Paul and Y. Yampol'skii, CRC press, Boca Raton, 1994.
- 28 R. Spillman, *Chem. Eng. Prog.*, 1989, **85**, 41–62.
- 29 B. D. Freeman, *Macromolecules*, 1999, **32**, 375–380.
- 30 R. S. Kohn, S. R. Jones and W. H. Mueller, *US pat.*, 5074891, 1991.
- 31 W. M. Lee, *Polym. Eng. Sci.*, 1980, **20**, 65–79.
- 32 A. Bondi, *J. Phys. Chem.*, 1964, **68**, 441–451.
- 33 D. W. van Krevelen, in *Properties of Polymers: their Correlation with Chemical Structure, their Numerical Estimation and Prediction from Additive Group Contributions*, Elsevier, Amsterdam, Netherlands, 1990.
- 34 A. Thran, G. Kroll and F. Faupel, *J. Polym. Sci., Part B: Polym. Phys.*, 1999, **37**, 3344–3358.
- 35 P. M. Budd, N. B. McKeown and D. Fritsch, *J. Mater. Chem.*, 2005, **15**, 1977–1986.
- 36 R. A. Hayes, *US pat.*, 5076817, 1991.
- 37 M. Langsam, *Plast. Eng.*, 1996, **36**, 697–741.
- 38 S. A. Stern, *J. Membr. Sci.*, 1994, **94**, 1–65.
- 39 H. N. Beck, E. S. J. Sanders and G. G. Lipscomb, *US pat.*, 4962131, 1990.
- 40 N. Chen, C. F. Tien and S. M. Patton, *US pat.*, 5232471, 1993.
- 41 B. W. Laverty, R. Vujosevic, S. Dang, B. Yao, T. Matsuura and G. Chowdhury, GB 2334526, 1999.
- 42 H. Lin and B. D. Freeman, *J. Membr. Sci.*, 2004, **239**, 105–117.
- 43 H. Hachisuga, *JP pat.*, 11342322, 1999.
- 44 (a) B. Bikson, M. J. Coplan and G. Goetz, *US pat.*, 4508852, 1985; (b) M. J. Coplan, C. H. Park and S. C. Williams, *US pat.*, 4414368, 1983; (c) J. B. Rose, *US pat.*, 4268650, 1981; (d) J. H. Kawakami, B. Bikson, G. Gotz and Y. Ozcaayir, *EP pat.*, 0426118, 1991.
- 45 W. J. Koros and D. R. B. Walker, *US pat.*, 5262056, 1993.
- 46 S. Kazama, S. Morimoto, S. Tanaka, H. Mano, T. Yashima, K. Yamada and K. Haraya, Cardo Polyimide Membranes for CO<sub>2</sub> Capture from Flue Gases, in *Proceedings of Seventh International Conference on Greenhouse Gas Control Technologies*, ed. E. S. Rubin, D. W. Keith and C. F. Gilboy, Cheltenham, UK, 2004.
- 47 R. Baker, *CO<sub>2</sub> Separation and Sequestration from Flue Gas with Membranes*, Post-Combustion CO<sub>2</sub> Capture Workshop, Talloires, France, July 11, 2010.
- 48 W. Yave, A. Car, S. S. Funari, S. P. Nunes and K.-V. Peinemann, *Macromolecules*, 2010, **43**, 326–333.
- 49 M. L. Cecopieri-Gomez, J. Palacios-Alquisira and J. M. Dominguez, *J. Membr. Sci.*, 2007, **293**, 53–65.
- 50 J. D. Wind, D. R. Paul and W. J. Koros, *J. Membr. Sci.*, 2004, **228**, 227–236.
- 51 A. M. W. Hillock and W. J. Koros, *Macromolecules*, 2007, **40**, 583–587.
- 52 Y. Xiao, B. Low, S. S. Hosseini, T.-S. Chung and D. R. Paul, *Prog. Polym. Sci.*, 2009, **34**, 561–580.
- 53 K. Tanaka, H. Kita, M. Okano and K. I. Okamoto, *Polymer*, 1992, **33**, 585–592.
- 54 M. R. Coleman and W. J. Koros, *J. Membr. Sci.*, 1990, **50**, 285–297.
- 55 Y. Liu, C. Pan, M. Ding and J. Xu, *Polym. Int.*, 1999, **48**, 832–836.
- 56 W. H. Lin, R. H. Vora and T.-S. Chung, *J. Polym. Sci., Part B: Polym. Phys.*, 2000, **38**, 2703–2713.
- 57 C. Nagel, K. Guenther-Schade, D. Fritsch, T. Strunskus and F. Faupel, *Macromolecules*, 2002, **35**, 2071–2077.
- 58 D. Hofman, J. Ulbrich, D. Fritsch and D. Paul, *Polymer*, 1996, **37**, 4773–4785.
- 59 B. S. Ghanem, N. B. McKeown, P. M. Budd, J. D. Selbie and D. Fritsch, *Adv. Mater.*, 2008, **20**, 2766–2771.
- 60 B. S. Ghanem, N. B. McKeown, P. M. Budd, N. M. Al-Harbi, D. Fritsch, K. Heinrich, L. Starannikova, A. Tokarev and Y. Yampol'skii, *Macromolecules*, 2009, **42**, 7881–7888.
- 61 J. Weber, Q. Su, M. Antonietti and A. Thomas, *Macromol. Rapid Commun.*, 2007, **28**, 1871–1876.
- 62 S. K. Sen and S. Banerjee, *J. Membr. Sci.*, 2010, **365**, 329–340.
- 63 Y. Hirayama, S. Kazama, E. Fujisawa, M. Nakabayashi, N. Matsumiya, K. Takagi, K. Okabe, H. Mano, K. Haray and C. Kamizawa, *Energy Convers. Manage.*, 1995, **36**, 435–438.
- 64 Y. J. Cho and H. B. Park, *Macromol. Rapid Commun.*, 2011, **32**, 579–586.
- 65 M. S. Boroglu and M. A. Gurkaynaka, *Polym. Adv. Technol.*, 2011, **22**, 545–553.
- 66 M. Calle, A. E. Lozano, J. G. Campa and J. Abajo, *Macromolecules*, 2010, **43**, 2268–2275.
- 67 G. L. Tullios, J. M. Powers, S. J. Jeskey and L. J. Mathias, *Macromolecules*, 1999, **32**, 3598–3612.
- 68 G. L. Tullios and L. J. Mathias, *Polymer*, 1999, **40**, 3463–3468.



- 69 A. M. Kratochvil and W. J. Koros, *Macromolecules*, 2008, **41**, 7920–7927.
- 70 B. T. Low, T.-S. Chung, H. Chen, Y. Jean and K. P. Pramoda, *Macromolecules*, 2009, **42**, 7042–7054.
- 71 C. M. Zimmerman and W. J. Koros, *J. Polym. Sci., Part B: Polym. Phys.*, 1999, **37**, 1235–1249.
- 72 D. R. B. Walker and W. J. Koros, *J. Membr. Sci.*, 1991, **55**, 99–117.
- 73 C. M. Zimmerman and W. J. Koros, *J. Polym. Sci., Part B: Polym. Phys.*, 1999, **37**, 1251–1265.
- 74 K. Tanaka, M. Okano, H. Toshino, H. Kita and K.-I. Okamoto, *J. Polym. Sci., Part B: Polym. Phys.*, 1992, **30**, 907–914.
- 75 M. Al-Masei, D. Fritsch and H. R. Kricheldorf, *Macromolecules*, 2000, **33**, 7127–7135.
- 76 J. de Abajo, J. G. de la Campa, A. E. Lozano, J. Espeso and C. Garcia, *Macromol. Symp.*, 2003, **199**, 293–305.
- 77 M. Al-Masei, H. R. Kricheldorf and D. Fritsch, *Macromolecules*, 1999, **32**, 7853–7858.
- 78 H. B. Park, C. H. Jung, Y. M. Lee, A. J. Hill, S. J. Pas, S. T. Mudie, E. van Wagner, B. D. Freeman and D. J. Cookson, *Science*, 2007, **318**, 254–258.
- 79 H. B. Park, S. H. Han, C. H. Jung, Y. M. Lee and A. J. Hill, *J. Membr. Sci.*, 2010, **359**, 11–24.
- 80 C. H. Jung, J. E. Lee, S. H. Han, H. B. Park and Y. M. Lee, *J. Membr. Sci.*, 2010, **350**, 301–309.
- 81 J. I. Choi, C. H. Jung, S. H. Han, H. B. Park and Y. M. Lee, *J. Membr. Sci.*, 2010, **349**, 358–368.
- 82 S. H. Han, J. E. Lee, K.-J. Lee, H. B. Park and Y. M. Lee, *J. Membr. Sci.*, 2010, **357**, 143–151.
- 83 T. Masuda, *J. Polym. Sci., Part A: Polym. Chem.*, 2007, **45**, 165–180.
- 84 V. S. Khotimsky, M. V. Tchirkova, E. G. Litvinova, A. I. Rebrov and G. N. Bondarenko, *J. Polym. Sci., Part A: Polym. Chem.*, 2003, **41**, 2133–2155.
- 85 J. Jia and G. L. Baker, *J. Polym. Sci., Part B: Polym. Phys.*, 1998, **36**, 959–968.
- 86 L. M. Robeson, W. F. Burgoyne, M. Langsam, A. C. Savoca, C. F. Tien, *Polymer*, 1994, **35**, 4970–4978.
- 87 T. Masuda, E. Isobe, T. Higashimura and K. Takada, *J. Am. Chem. Soc.*, 1983, **105**, 7473–7474.
- 88 T. Aoki, *Prog. Polym. Sci.*, 1999, **24**, 951–993.
- 89 M. Ulbricht, *Polymer*, 2006, **47**, 2217–2262.
- 90 K. Nagai, T. Masuda, T. Nakagawa, B. D. Freeman and I. Pinnau, *Prog. Polym. Sci.*, 2001, **26**, 721–797.
- 91 H. Kouzai, T. Masuda and T. Higashimura, *J. Polym. Sci., Part A: Polym. Chem.*, 1994, **32**, 2523–2530.
- 92 H. Tachimori and T. Masuda, *J. Polym. Sci., Part A: Polym. Chem.*, 1995, **33**, 2079–2085.
- 93 Y. Hu, M. Shiotsuki, F. Sanda, B. D. Freeman and T. Masuda, *Macromolecules*, 2008, **41**, 8525–8532.
- 94 Y. Ichiraku, S. A. Stern and T. Nakagawa, *J. Membr. Sci.*, 1987, **34**, 5–18.
- 95 K. Nagai, A. Higuchi and T. Nakagawa, *J. Polym. Sci., Part B: Polym. Phys.*, 1995, **33**, 289–298.
- 96 S. D. Kelman, S. Matteucci, C. W. Bielawski and B. D. Freeman, *Polymer*, 2007, **48**, 6881–6892.
- 97 N. B. McKeown, S. Makhseed and P. M. Budd, *Chem. Commun.*, 2002, 2780–2781.
- 98 N. B. McKeown, S. Hanif, K. Msayib, C. E. Tattershall and P. M. Budd, *Chem. Commun.*, 2002, 2782–2783.
- 99 P. M. Budd, B. S. Ghanem, S. Makhseed, N. B. McKeown, K. J. Msayib and C. E. Tattershall, *Chem. Commun.*, 2004, 230–231.
- 100 P. M. Budd, E. S. Elabas, B. S. Ghanem, S. Makhseed, N. B. McKeown, K. J. Msayib, C. E. Tattershall and D. Wang, *Adv. Mater.*, 2004, **16**, 456–459.
- 101 J. Song, N. Du, Y. Dai, G. P. Robertson, M. D. Guiver, S. Thomas and I. Pinnau, *Macromolecules*, 2008, **41**, 7411–7417.
- 102 N. Du, J. Song, G. P. Robertson, I. Pinnau and M. D. Guiver, *Macromol. Rapid Commun.*, 2008, **29**, 783–788.
- 103 N. B. McKeown and P. M. Budd, *Chem. Soc. Rev.*, 2006, **35**, 675–683.
- 104 P. M. Budd and N. B. McKeown, *Polym. Chem.*, 2010, **1**, 63–68.
- 105 P. M. Budd, N. B. McKeown, B. S. Ghanem, K. J. Msayib, D. Fritsch, L. Starannikova, N. Belov, O. Sanfirova, Y. Yampolskii and V. Shantarovich, *J. Membr. Sci.*, 2008, **325**, 851–860.
- 106 N. Du, G. P. Robertson, I. Pinnau and M. D. Guiver, *Macromolecules*, 2009, **42**, 6023–6030.
- 107 N. Du, G. P. Robertson, I. Pinnau and M. D. Guiver, *Macromolecules*, 2010, **43**, 8580–8587.
- 108 T. Emmler, K. Heinrich, D. Fritsch, P. M. Budd, N. Chaukura, D. Ehlers, K. Ratzke and F. Faupel, *Macromolecules*, 2010, **43**, 6075–6084.
- 109 B. S. Ghanem, N. B. McKeown, P. M. Budd and D. Fritsch, *Macromolecules*, 2008, **41**, 1640–1646.
- 110 P. M. Budd, N. B. McKeown and D. Fritsch, *Macromol. Symp.*, 2006, **245–246**, 403–405.
- 111 N. Du, G. P. Robertson, I. Pinnau, S. Thomas and M. D. Guiver, *Macromol. Rapid Commun.*, 2009, **30**, 584–588.
- 112 M. Carta, K. J. Msayib, P. M. Budd and N. B. McKeown, *Org. Lett.*, 2008, **10**, 2641–2643.
- 113 M. Carta, K. J. Msayib and N. B. McKeown, *Tetrahedron Lett.*, 2009, **50**, 5954–5957.
- 114 R. Short, M. Carta, C. G. Bezzu, D. Fritsch, B. M. Kariuki and N. B. McKeown, *Chem. Commun.*, 2011, **47**, 6822–6824.
- 115 N. Du, G. P. Robertson, J. Song, I. Pinnau and M. D. Guiver, *Macromolecules*, 2009, **42**, 6038–6043.
- 116 N. Du, G. P. Robertson, J. Song, I. Pinnau, S. Thomas and M. D. Guiver, *Macromolecules*, 2008, **41**, 9656–9662.
- 117 D. Fritsch, G. Bengtson, M. Carta and N. B. McKeown, *Macromol. Chem. Phys.*, 2011, **212**, 1137–1146.
- 118 N. Du, H. B. Park, G. P. Robertson, M. M. Dal-Cin, T. Visser, L. Scoles and M. D. Guiver, *Nat. Mater.*, 2011, **10**, 372–375.
- 119 N. Du, M. M. Dal-Cin, I. Pinnau, A. Nicalek, G. P. Robertson and M. D. Guiver, *Macromol. Rapid Commun.*, 2011, **32**, 631–636.
- 120 P. M. Budd, K. J. Msayib, C. E. Tattershall, B. S. Ghanem, K. J. Reynolds, N. B. McKeown and D. Fritsch, *J. Membr. Sci.*, 2005, **251**, 263–269.
- 121 T. Sarbu, T. Styranc and E. J. Beckmann, *Nature*, 2000, **405**, 165–168.
- 122 H. Lin and B. D. Freeman, *J. Mol. Struct.*, 2005, **739**, 57–74.
- 123 H. Lin, E. van Wagner, B. D. Freeman, L. G. Toy and R. P. Gupta, *Science*, 2006, **311**, 639–642.
- 124 H. Lin, E. van Wagner, J. S. Swinnea, B. D. Freeman, S. J. Pas, A. J. Hill, S. Kalakkunnath and D. S. Kalika, *J. Membr. Sci.*, 2006, **276**, 145–161.
- 125 M. Yoshino, K. Ito, H. Kita and K.-I. Okamoto, *J. Polym. Sci., Part B: Polym. Phys.*, 2000, **38**, 1707–1715.
- 126 V. I. Bondar, B. D. Freeman and I. Pinnau, *J. Polym. Sci., Part B: Polym. Phys.*, 2000, **38**, 2051–2062.
- 127 K. Okamoto, M. Fujii, S. Okamoto, H. Suzuki, K. Tanaka and H. Kita, *Macromolecules*, 1995, **28**, 6950–6956.
- 128 H. W. Kim and H. B. Park, *J. Membr. Sci.*, 2011, **372**, 116–124.
- 129 J. Potreck, K. Nijmeijer, T. Kosinski and M. Wessling, *J. Membr. Sci.*, 2009, **338**, 11–16.
- 130 S. R. Reijerkerk, M. H. Knoef, K. Nijmeijer and M. Wessling, *J. Membr. Sci.*, 2010, **352**, 126–135.
- 131 S. R. Reijerkerk, A. C. IJzer, K. Nijmeijer, A. Arun, R. J. Gaymans and M. Wessling, *ACS Appl. Mater. Interfaces*, 2010, **2**, 551–560.
- 132 S. R. Reijerkerk, M. Wessling and K. Nijmeijer, *J. Membr. Sci.*, 2011, **378**, 479–484.
- 133 H. Lin, E. van Wagner, R. Raharjo, B. D. Freeman and I. Roman, *Adv. Mater.*, 2006, **18**, 39–44.
- 134 H. Lin, E. van Wagner, B. D. Freeman, L. G. Toy and R. P. Gupta, *Science*, 2006, **311**, 639–642.
- 135 Y. Hirayama, Y. Kase, N. Tanihara, Y. Sumiyama, Y. Kusuki and K. Haraya, *J. Membr. Sci.*, 1999, **160**, 87–99.